https://doi.org/10.5194/egusphere-2026-2492
Preprint. Discussion started: 10 June 2026

Modular Hardware and Software System for Multi-Sensor Environment Perception (MOSEP)

Christoph Gaisberger[1], Stefan Muckenhuber[1,2,3], Birgit Schlager[1,3], Thomas Goelles[1,3], Simon Genser[3], Markus Schratter[3], and Wolfgang Schöner[1]

[1]Department of Geography and Regional Science, University of Graz, 8010 Graz, Austria
[2]Institute of Industrial Management, FH Joanneum Graz, 8605 Kapfenberg, Austria
[3]Virtual Vehicle Research GmbH, 8010 Graz, Austria

Correspondence: Christoph Gaisberger (christoph.gaisberger@uni-graz.at)

Abstract. Dynamic environmental processes, from landslides and avalanches to river channel migration and glacier calving, demand innovative monitoring solutions that offer both high spatial and temporal resolution while being robust and cost-effective. Recent advances in robotics and autonomous systems have introduced a new generation of perception sensors, including lidar, radar, and cameras, that have the potential to transform environmental monitoring. While these technologies have long been applied in science, they have traditionally been highly specialized, costly, and designed for narrow use cases. This paper investigates the capabilities of emerging low-cost, lightweight perception sensors for environmental monitoring, including meteorological applications. We introduce the Modular Hardware and Software System for Multi-Sensor Environment Perception (MOSEP), an adaptable and portable hardware platform complemented by a fully open-source software stack that enables time-synchronous collection of multi-sensor data. MOSEP integrates automotive-grade perception sensors with meteorological instruments, offering a temporal resolution of up to 20 Hz and a range of several hundred meters. The system's robustness and flexibility were validated in real-world scenarios, including stationary deployments and mobile data acquisition on land and sea, such as for iceberg mapping in East Greenland. This paper details the design, integration, and capabilities of the MOSEP platform, showcasing its scalability and adaptability. The results underscore the utility of MOSEP as a versatile tool for environmental sensing, with broad applications in geoscience and other fields. By providing a reproducible, open-source platform, this work aims to motivate researchers to adopt these emerging sensor technologies for their own applications.

1 Introduction

Autonomous systems have recently become central to innovation across a wide range of research fields, particularly in the robotics and automotive industries. In addition, semi-autonomous and remote control systems, such as Unmanned Aircraft Systems (UASs), are increasingly being used for new applications, including environmental research. These advancements have been enabled by a new generation of low-cost perception sensors, including Light Detection and Ranging (lidar), radar, and time-of-flight (TOF) cameras. Further innovative and inexpensive sensor systems are expected to enter the market in the coming years, such as solid-state lidar, 4D radar, and requency Modulated Continuous Wave (FMCW) lidar. The automotive industry, in particular, has driven the development of new sensors with ongoing improvements in accuracy, size, and cost for

https://doi.org/10.5194/egusphere-2026-2492
Preprint. Discussion started: 10 June 2026

assisted and autonomous driving (Watzenig and Horn, 2017). Consequently, these new sensor devices are also being exploited for scientific applications in environmental monitoring. These new systems provide a multitude of new opportunities, not only in advanced use cases involving autonomous UASs mapping but also for more traditional monitoring applications. The high temporal resolution of automotive sensors enables the observation of rapid environmental changes, offering an affordable and effective alternative to traditional geophysical sensors like Terrestrial Laser Scanner (TLS). This is particularly true when considering the additional benefits of sensor fusion, which is the process of combining data from multiple sensors to achieve more accurate, complete and robust information. To achive this we are introducing Modular Hardware and Software System for Multi-Sensor Environment Perception (MOSEP). This new system offers flexibility, mobility, and high temporal resolution (about 10 Hz, depending on the integrated sensor systems), with a range of up to a few hundred meters. These capabilities are particularly advantageous for studying small-scale features and fast processes that are otherwise difficult to capture with traditional monitoring systems, which either cannot be installed permanently or are based on aerial or satellite remote sensing with coarser resolution and infrequent revisit times. However, a thorough evaluation of the performance, data quality, and limitations of this new generation of low-cost perception sensors is required. Moreover, since these sensors are typically not standalone, plug-and-play systems, a flexible and modular hardware integration is necessary to enable multi-sensor fusion and support their application in new research fields. To address these challenges, we developed a versatile platform that enables simple hardware and software integration of new sensors. The system is based on the cost-effective Raspberry Pi computer and the Robot Operating System (ROS), a Free and Open Source Software (FOSS) software ecosystem for integrating sensors, synchronizing data streams, recording measurements, and controlling devices (Open Robotics, 2025a).

We distinguish between two primary applications: mapping and monitoring. Mapping typically involves moving the sensor platform through a generally static environment to create a spatially accurate representation. This process enables the creation of comprehensive 3D models, as the system collects spatial data in a single pass or over a short period. In contrast, monitoring focuses on the continuous or periodic observation of dynamic processes over time, often with the sensor deployed in a fixed location or repeatedly visiting the same locations. This approach allows for the observation and recording of environmental changes, making it essential for applications that require real-time or long-term data on evolving conditions.

In recent years, there has been a growing effort to repurpose sensors originally developed for autonomous systems for environmental data acquisition. Among these, lidar has become particularly popular. For example, Dharmadasa et al. (2022) and Jacobs et al. (2021) used UAS-lidar for snow depth measurements, while Rauhala et al. (2023) found lidar to be superior to Structure from motion (SfM) for mapping homogeneous textures and for tree canopy penetration. In a previous study, we used a subsystem of the platform presented here to measure snow depth from a cable car with lidar at Hoher Sonnblick, Austria, achieving cm-level precision (Dikic et al., 2026). New sensor technologies are also widely used in fields with a strong remote sensing tradition, such as ecology, forestry, and agriculture, often deployed on UASs (Van Alphen et al., 2024; Hu et al., 2021; Christiansen et al., 2017; Raman et al., 2022; Renette et al., 2024; Výbošťok et al., 2025), but also on handheld devices (Hyyppä et al., 2020). In disaster management, lidar-based UAS systems have also shown promising results for environmental reconstruction (Chiang et al., 2017). However, far fewer studies have investigated static platforms using the new generation of perception sensors and sensor fusion for environmental monitoring. Existing work includes Perks et al. (2024) who use

https://doi.org/10.5194/egusphere-2026-2492
Preprint. Discussion started: 10 June 2026

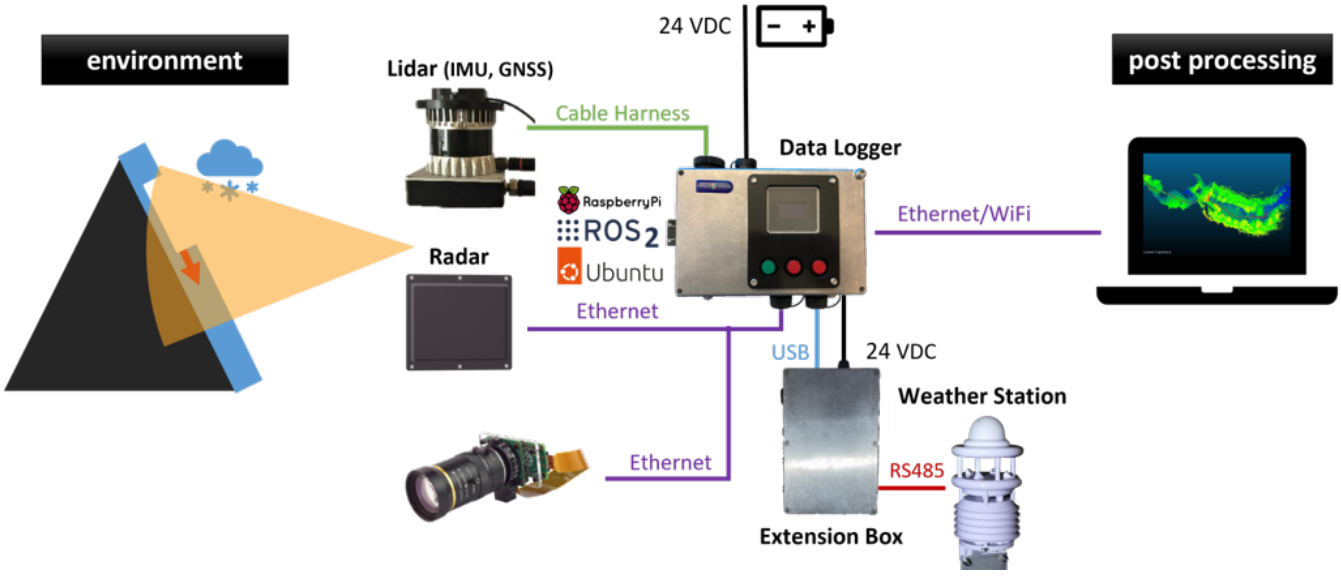

Figure 1. Schematic view of MOSEP including perception sensors lidar, radar, camera and a weather station.

lidar to assess hydrogeomorphic changes on riverbanks, Aaron et al. (2023) measure debris-flow parameters such as velocity and particle trajectory, Garcia-Sellés et al. (2023) continuously monitor for rock falls and Ruttner-Jansen et al. (2024) perform snow depth monitoring in the Swiss Alps. Although photogrammetric approaches using UASs can outperform inexpensive lidar systems in terms of accuracy (Štroner et al., 2023), they require multiple images acquired from different viewing angles and prominent surface features to achieve high quality reconstructions. Fixed camera systems for continuous monitoring would likewise require multiple installations and would probably still provide lower accuracy than fixed lidar systems (Filhol et al., 2019). In addition, UASs depend on suitable weather conditions, require a trained operator, and are subject to airspace restrictions. In this paper, we address this gap by presenting our experience with a new generation of perception sensors in both terrestrial and marine applications. We provide a detailed hardware and software stack to facilitate replication and offer inspiration for future applications.

1.1 Motivation

This work builds on the experiences and knowledge that we gathered during the development of MObile LIdar SENsor System (MOLISENS) (Goelles et al., 2022). Previous research demonstrated that MOLISENS can perform short range (order of 100m) mapping tasks with multiple acquisition positions (e.g. in caves) more efficiently than conventional TLS while maintaining adequate accuracy at about one-tenth of the cost. Meanwhile, the industry has introduced several ready-to-use alternatives (e.g., YellowScan - Surveyor Ultra (YellowScan, 2025), Viametris - MS-96 (Viametris, 2025), Aerial Precision - AP-LiDAR-One (Aerial Precision, 2025), SATLAB - Cygnus (SATLAB, 2025), etc.) that, despite their reduced flexibility, underscore the growing interest in mobile scanning technologies. At the same time, new research questions have emerged within our

https://doi.org/10.5194/egusphere-2026-2492
Preprint. Discussion started: 10 June 2026

group, particularly those related to atmospheric processes, snow dynamics, and mass movements. This type of research often takes place in remote, hard-to-reach locations, createing the need for a self-sufficient, autonomous system. In conjunction with recent advancements in sensor capabilities and the anticipation of future sensor technologies (e.g., 4D radar, FMCW lidar), our research focus has broadened from mobile mapping to continuous, multi-purpose environmental monitoring. This transition has motivated the development of an updated, integrated sensing platform with evolved objectives and design priorities. Typically, perception sensors are not designed for standalone application but are instead integrated into a carrier platform (e.g., car, train or UAS). Moreover, integrating multiple sensors with different communication and power standards presents challenges, but combining them into a single system also offers several advantages over operating them individually:

- **Single database:** Recording data from all sensors into one database simplifies analysis by providing a unified API, a consistent data structure, and streamlined querying.
- **Time-synchronous recording:** Coordinating data collection via a common communication model ensures that all sensor outputs are time-synchronized, eliminating the need for data alignment during post-processing.
- **Single power supply:** Since these sensors generally lack independent power sources but have similar power requirements, integrating them allows for a common power solution (whether battery- or grid-powered).

For a sensing system to be truly versatile and autonomous, it must operate reliably under diverse weather conditions (e.g., hot, cold, wet, dusty). Accordingly, the hardware must be waterproof, dustproof, and capable of withstanding extreme temperatures, while sensors should ideally operate reliably regardless of environmental conditions. Additionally, sensor performance in adverse weather is of great interest and a major field of research in the automotive industry and for (semi-)autonomous and remote control systems in general. As continuous environmental monitoring has to deal with similar challenges, evaluating atmospheric influences is among the major motivations for this research. Ultimately, this research aims to help establish a foundation for future monitoring efforts, with potential applications spanning geosciences, including snow avalanche, landslide, and weather monitoring.

In reality, perception sensors are strongly influenced by adverse weather (Zhang et al., 2021; Kutila et al., 2018; Jokela et al., 2019), and therefore it is important to know their performance limitations in such conditions. Protecting the hardware from the elements is the first step and sensors developed for the automotive industry prove to be an ideal fit, since they are built for all weather conditions and are usually rated IP68 and above. For the data logging component, an efficient computing platform is essential, not only to conserve energy and extend battery life for remote deployments, but also to minimize heat generation. A system that functions without active cooling can be fully sealed within a waterproof enclosure. Conversely, in cold conditions it can be beneficial to have some heat-generating components to prevent damage.

To achieve the above mentioned challenges, we developed a new modular, multi-sensor platform, transitioning the approach from a mobile lidar system mapping a static scene to a versatile, multi-sensor system that allows monitoring a dynamic environment both from a fixed or moving observation point. The hardware and software capabilities have been developed to support a flexible configuration that facilitates the integration of several different (and newly emerging) sensor systems, including lidar,

https://doi.org/10.5194/egusphere-2026-2492
Preprint. Discussion started: 10 June 2026

radar, camera, meteorological sensors, etc. The new platform was tested under a variety of scenarios and a number of datasets were acquired with three examples presented in Chapter 3.

The following sections provide a brief overview of the lessons learned during the MOLISENS development and a detailed description of the new sensor platform. After that, we demonstrate three example use cases where the new system was successfully used.

1.2 System background

The sensor system MOLISENS was primarily designed for lidar mapping applications. It was built around an Ouster lidar sensor with a 360-degree horizontal field of view and included a Global Navigation Satellite System (GNSS) module and an Inertial Measurement Unit (IMU) for Simultaneous Localization And Mapping (SLAM). The computing unit, along with communication and power transformation components were housed in a compact aluminum enclosure that facilitated connections to both the sensor unit and external batteries. Since some heat generation is unavoidable, all heat-generating components are mounted on aluminum plates connected to the aluminum housing, which acts as a large heat spreader (compare 3). The system was intentionally designed to be lightweight and portable, enabling environmental mapping applications in remote and/or difficult-to-access areas. To generate coherent maps from individual lidar point clouds, the open-source SLAM algorithm LIO-SAM was used. The system was extensively tested on multiple occasions in various applications, including two mapping campaigns in the Lurgrotte cave, Austria and a glacier cave on Longyearbreen, Svalbard (Goelles et al., 2022).

While system compactness remains a priority, given the need for transportation to remote operating sites, sometimes by foot, additional requirements have emerged due to the stationary and long-term nature of monitoring. Power efficiency and thermal management are similarly important as in mapping applications, but the shift to a permanently installed setup that should reliably operate without intervention for extended periods introduces new requirements for hardware and software. To support sustained operation, remote access is crucial for system monitoring and troubleshooting. Moreover, because perception sensors like lidar generate large volumes of data that can quickly consume storage, implementing automated recording mechanisms that capture only relevant temporal and spatial segments is essential to optimize data storage and relevance.

2 MOSEP sensor platform

A crucial part of every sensor platform is to support common standards for data transmission from sensors. Currently, there is no unified standard for environmental perception sensor data communication; however, some commonalities exist. Common hardware interfaces include SDI-12, RS-232, or RS-485, all of which can easily be adapted to USB via compact converters. Fortunately, most perception sensors feature an Ethernet interface, greatly simplifying their integration and control. Power delivery is another critical consideration.

In the current MOSEP system, all integrated sensors operate at 24 V, although additional voltage levels can be accommodated with minimal modifications. A schematic overview of the system is depicted in Fig. 1. To handle the diverse data formats and communication protocols of the incorporated sensors, we utilize ROS, a FOSS software stack widely employed in robotics

https://doi.org/10.5194/egusphere-2026-2492
Preprint. Discussion started: 10 June 2026

Table 1. Sensors integrated and tested with MOSEP and their specifications according to the datasheets.

Sensor	Model	Update Rate	Resolution	Spectrum	Interface	Power Supply	Range	Accuracy[a]
Lidar	Ouster OS1/OS2	up to 20 Hz	0.1 cm[b]	865 nm	RJ45	24 VDC@20 W/24 W	100/210 m[c]	±3 cm
Radar	Smartm. UMRR-11	up to 20 Hz	–	77 GHz	RJ45	8-32 VDC@5 W	175 m	<0.5 m
Camera	Raspberry Pi HQ	up to 120 Hz	12.3 MP	Vis. Light	RJ45	5 VDC@6 W	Optics Ltd.[d]	–
WS	Lufft WS100	1 Hz	–	24 GHz	RS-485	10-28 VDC@10 W	–	–
WS	Lufft WS501-UMB	1 Hz	–	–	RS-485	24 VDC@25 W	–	–
IMU	Xsens MTi-630	up to 400 Hz	–	–	USB	5 VDC@0.5 W	–	–
GNSS	u-blox ZED-F9R	1 Hz	–	–	UART	3.3 VDC@0.33 W	–	±1 cm[e]

[a] Refers to Range Accuracy for active sensors (Lidar/Radar) and Position Accuracy for GNSS.
[b] Range resolution.
[c] For an 80% Lambertian reflective target.
[d] Limited by sensor resolution, lens focal length, and ambient light.
[e] Horizontal position accuracy (without RTK).

and autonomous systems. ROS simplifies the integration process by providing sensor drivers for efficient data handling and standardized communication. It features a publisher-subscriber (pub/sub) model for sensor communication with the central coordination instance and facilitates time-synchronous recording of data streams from all sensors into a unified database, known as a 'ROS bag file', and saved in mcap format (Open Robotics, 2025b; Foxglove, 2025). This multivariate time series can then later be loaded, analyzed and exported.

2.1 Sensors

The MOSEP platform is compatible with a wide range of environmental perception and meteorological sensors (hereafter collectively referred to as environmental sensors). For the demonstration campaigns described herein, a specific set of sensors was used, comprising a lidar, radar, camera, two Weather Stations (WSs), a GNSS receiver, and an IMU. A summary of the tested devices is provided in Table 1.

Lidar

lidar sensors available today broadly fall into three categories: consumer-grade, low-cost, and professional-grade. Consumer-grade lidar sensors, such as those integrated into smartphones like the iPhone 15 Pro (King et al., 2023), typically cost only a few euros but have limited ranges of just a few meters. Low-cost systems from manufacturers such as Ouster or Livox, priced between several hundred to several tousand EUR, provide considerably longer sensing ranges (tens to hundreds of meters) along with sufficient accuracy for many environmental monitoring applications. In contrast, professional-grade TLS, such as those produced by Riegl, offer extremely high accuracy, longer ranges (up to several kilometers), and full-waveform capabilities, but they are substantially more expensive, often exceeding 100,000 EUR. Additionally, low-cost automotive lidar sensors offer a significant advantage over professional-grade TLS due to their high temporal resolution (typically 10-20 Hz), enabling detailed monitoring of rapidly changing environments. In this study, we explicitly focus on low-cost lidar sensors as they

https://doi.org/10.5194/egusphere-2026-2492
Preprint. Discussion started: 10 June 2026

provide an optimal balance between affordability and performance. Their moderate cost makes them suitable for permanent installations or extensive spatial coverage through multi-sensor deployments. At the same time, their range and high temporal resolution allow effective monitoring of environmental processes, such as snow surface dynamics, over distances of several hundred meters. The recent reduction in size, price, and complexity of low-cost lidar sensors has significantly contributed to their increasing adoption for environmental monitoring. For this study, two automotive lidar models from Ouster were used: the OS1 Rev6 and OS2 Rev5 (Ouster, 2025). Although these devices were not specifically designed for environmental monitoring, they have proven to be very effective across a wide range of applications. Operating at a wavelength of $865\,\mathrm{nm}$ they offer good reflectivity for surfaces such as ice and snow (Hotaling et al., 2021; Deems et al., 2013; Ji et al., 2022). Unlike specialized TLS, these devices typically record only one to three of the strongest returns, or the strongest and the last return, and generally do not offer full-waveform capabilities - that is, recording the entire reflected signal intensity profile across all distances for each emitted laser pulse (McManamon, 2019). The primary differences between the two models lie in their vertical field-of-view- $45°$ for the OS1 and $22.5°$ for the OS2-and their sensing ranges, which are approximately $100\,\mathrm{m}$ and $210\,\mathrm{m}$, respectively (for an $80\,\%$ reflective target at $> 90\,\%$ detection probability). Both lidar models meet laser product class 1 standards, ensuring eye safety, and are designed to be water- and dust-proof, which are both mature limitation of classical TLS. Their relatively low cost ($5,000$-$20,000\,\mathrm{EUR}$), light weight ($0.45\,\mathrm{kg}$ and $1.1\,\mathrm{kg}$) and increased ruggedness (rated IP68) further distinguish them from TLS, albeit with the trade-off of considerably reduced sensing range and range accuracy (approximately $\pm 3\,\mathrm{cm}$). Notably, newer revision 7 models reportedly offer up to $350\,\mathrm{m}$ range and improved noise suppression (Ouster, 2024).

Radar

An automotive radar sensor, the Smartmicro UMRR-11 Type 132 (Smartmicro, 2021), operating in the 76 to $77\,\mathrm{GHz}$ frequency band, was also integrated. The Smartmicro UMRR-11 Type 132 represents one of the first commercially available automotive radar sensors that can detect radar clusters in 3D and offer access on radar cluster level and can be operated without vehicle data (speed, acceleration, etc.) integration. Previous automotive radar sensors typically only provided 2D object data and vehicle data integration was mandatory. The automotive radar sensor was included to assess its potential capabilities and limitations for environmental applications, particularly due to its robustness in adverse weather conditions such as rain, snow, or fog, where optical sensors like lidar and cameras may be limited. In long-range mode, where it can detect targets up to a range of approximately $175\,\mathrm{m}$, the radar provides a field of view of $\pm 16°$ in azimuth and $\pm 7.5°$ in elevation. The radars internal processor groups raw detections into clusters representing distinct objects. For each object, the radar provides its position, velocity (based on Doppler shift), and radar cross-section (RCS), which is a measure of the object's reflectivity. This pre-processing simplifies data analysis by providing a high-level representation of the scene, making it well-suited for object tracking and dynamic scene analysis. At the same time, by not providing raw doppler maps it obscures the underlying detection data, which can limit its use for applications requiring analysis of distributed targets, such as precipitation, or the development of custom detection algorithms. This is a common problem of many commercial products.

Camera

https://doi.org/10.5194/egusphere-2026-2492
Preprint. Discussion started: 10 June 2026

To integrate RGB images into the synchronous recording, the imaging device must support some form of live communication. Many DSLR cameras are suitable for this purpose, particularly if they are supported by the gphoto library[1], which enables remote control and image transfer. While DSLRs can provide superb image quality, they often come at a higher cost. Alternatively, IP cameras, which operate directly over an Ethernet connection, range from simple surveillance models to advanced industrial-grade systems. In view of the high cost of industrial IP cameras and DSLR solutions (often exceeding 1000 EUR), especially those with interchangeable lenses, and the limited flexibility of typical surveillance cameras, we used a custom camera system, assembled from off-the-shelf components. This system is based on the Raspberry Pi HQ Camera module, paired with a Raspberry Pi 4 (see Fig. 2), and costs approximately 100-150 EUR, excluding the housing (Raspberry Pi, 2025). The camera module is equipped with a 12.3-megapixel Sony IMX477 sensor and features a C/CS lens mount, allowing for the use of interchangeable lenses to suit different monitoring scenarios. Its back-illuminated sensor architecture enhances low-light performance and provides good light sensitivity for a sensor of its size, which is critical for environmental monitoring applications that often operate across day-night cycles. The system allows for manual control over key imaging parameters, including shutter speed, which can be adjusted from a few microseconds to several seconds (e.g., up to $200\,\mathrm{s}$), enabling long-exposure photography in dark conditions. While the maximum frame rate depends on the configured resolution, the system can deliver up to $10\text{-}11\,\mathrm{fps}$ at its full 4056x3040 resolution, which is sufficient for capturing many environmental processes. This combination of a high-quality sensor, lens flexibility, and software control provides a cost-effective yet powerful solution for visual environmental monitoring.

Weather Stations

To acquire meteorological data, two compact WSs from Lufft were used. The first unit, the WS501-UMB, is a general-purpose station measuring temperature, relative humidity, air pressure, wind direction, wind speed, and radiation OTT HydroMet (2024b). The second unit WS100, a $24\text{-}\mathrm{GHz}$ Doppler precipitation radar, is capable of measuring both liquid and solid precipitation amounts as well as identifying precipitation type (OTT HydroMet, 2024a). Both stations provide measurements at a rate of $1\,\mathrm{Hz}$. They comunicate via a proprietary binar protocoll called UMB over RS-485 and are usually connected to a standalone logger. To integrate them, a custom Robot Operating System 2 (ROS2) driver was created that translates the binary data, for use with any Lufft UMB weather station. The driver is available on GitHub (https://github.com/MOLISENS-MOSEP/drivers.lufft_weather_station) (Gaisberger, 2025).

GNSS and IMU

The platform also incorporates a GNSS receiver from u-blox (ZED-F9R) (ublox, 2023) with an option for Real-Time Kinematics (RTK) via LTE connectivity. This receiver supports all major satellite navigation systems and achieves a horizontal positional accuracy of approximately $\pm 1\,\mathrm{m}$ without RTK, improving to about $\pm 0.01\,\mathrm{m}$ with RTK under good conditions. The GNSS is complemented by a 9-axis IMU from Xsens (MTi-630) (Xsens, 2020), which provides a high temporal resolution of up to $400\,\mathrm{Hz}$. Both sensors were carried over from the legacy system and have been updated to ensure integration with the enhanced platform, as detailed in Goelles et al. (2022)

[1] a list of compatible models is available at http://www.gphoto.org/proj/libgphoto2/support.php

https://doi.org/10.5194/egusphere-2026-2492
Preprint. Discussion started: 10 June 2026

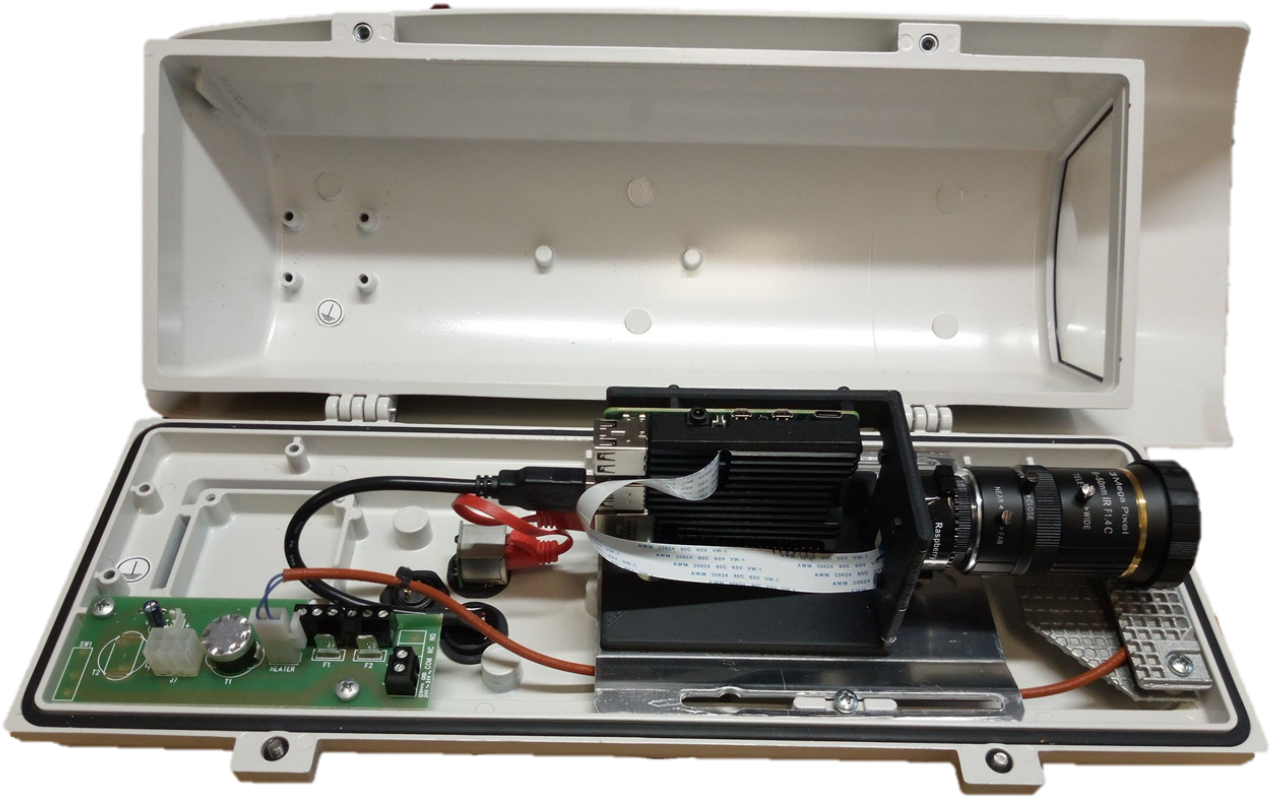

Figure 2. The camera system based on a Raspberry Pi HQ camera module with rainproof housing including an optional heater.

2.2 Logging and processing unit

The sensor platform is divided into two main components: a primary unit for data logging and power supply and an extension unit for additional connectivity. Both units can be operated independently. The primary unit encompasses a Raspberry Pi 4 Model B (4 GB RAM), serving as the central computing unit, alongside an SSD for data recording, an interface for the Ouster lidar, a GNSS module, an LTE modem, voltage converters, an Ethernet switch, and USB ports for maximum sensor communication flexibility. Engineered for durability, the entire assembly is rain- and dust-proof and can be powered through an external power source or 24-Volt batteries. The extension unit is designed to provide additional RS-485 connections, which is a very common interface for environmental sensors, the USB conversion components and a power supply. The extension unit can be used in addition to the primary unit or as a standalone adapter with any other computer via USB. A capable DC/DC converter (max 100 W) was included to account for the high power consumption of up to three, possibly heated, WS. A high-level block diagram is shown in Fig. 4. The use of standardized connectors and voltage levels ensure a highly modular design,

https://doi.org/10.5194/egusphere-2026-2492
Preprint. Discussion started: 10 June 2026

Table 2. Key hardware components of the MOSEP platform's primary unit (top) and extension unit (bottom). The listed parts represent a sample configuration and provide an overview of the components and associated costs. Note that the DC/DC converters are on the expensive side, as they were selected for high power efficiency, but they can be substituted with less expensive alternatives.

Part	Function	Model	approx. Price
01	Main processing unit	Raspberry Pi 4B/4GB	EUR 60
02	32GB SD Card	SandDisk Extreme	EUR 10
03	SATA SSD Hat	Geekworm X825	EUR 20
04	960GB SSD	Kingston A400	EUR 120
05	Real-Time-Clock	Raspberry Pi DS3231	EUR 5
06	LTE Stick	HUAWEI E3372h-320	EUR 60
07	DC/DC converter 24 V to 5 V	TracoPower TMDC 20-2411	EUR 70
08	24 V voltage regulator	TracoPower TEN 50-2415WI	EUR 110
09	GBit network switch	Renkforce	EUR 40
10	DC/DC converter 100 watt	Mean Well RSD-100B-24	EUR 65
11	DC/DC converter 24 V to 5 V	generic	EUR 5
12	4 Port USB Hub	generic	EUR 20
13	3x USB/RS-485 adapter	generic	EUR 10
14	Other small parts (cables, connectors, housing, etc.)	diverse	EUR 840
		rough total cost	EUR 1,435

allowing components to be easily reconfigured or replaced. Additionally, we employ a readily available, IP68-rated power connector (RS Components, 2025), which facilitates seamless integration with various sensing devices.

All components of the system are readily available off-the-shelf products (see Table 2 for a full list of parts). The Raspberry Pi as a processing unit was chosen due to its low price, low power consumption and its extensive ecosystem and software support. It is capable to run Ubuntu Server (necessary for ROS) while having enough headroom for data processing and operational logic.

2.3 Software

Integrating off-the-shelf perception sensors into scientific workflows often necessitates a trade-off between immediate utility and long-term flexibility. While manufacturer-provided proprietary software is typically optimized for reliability, its 'closed-box' nature can become a bottleneck when specialized needs arise-particularly regarding precise multi-sensor synchronization

https://doi.org/10.5194/egusphere-2026-2492
Preprint. Discussion started: 10 June 2026

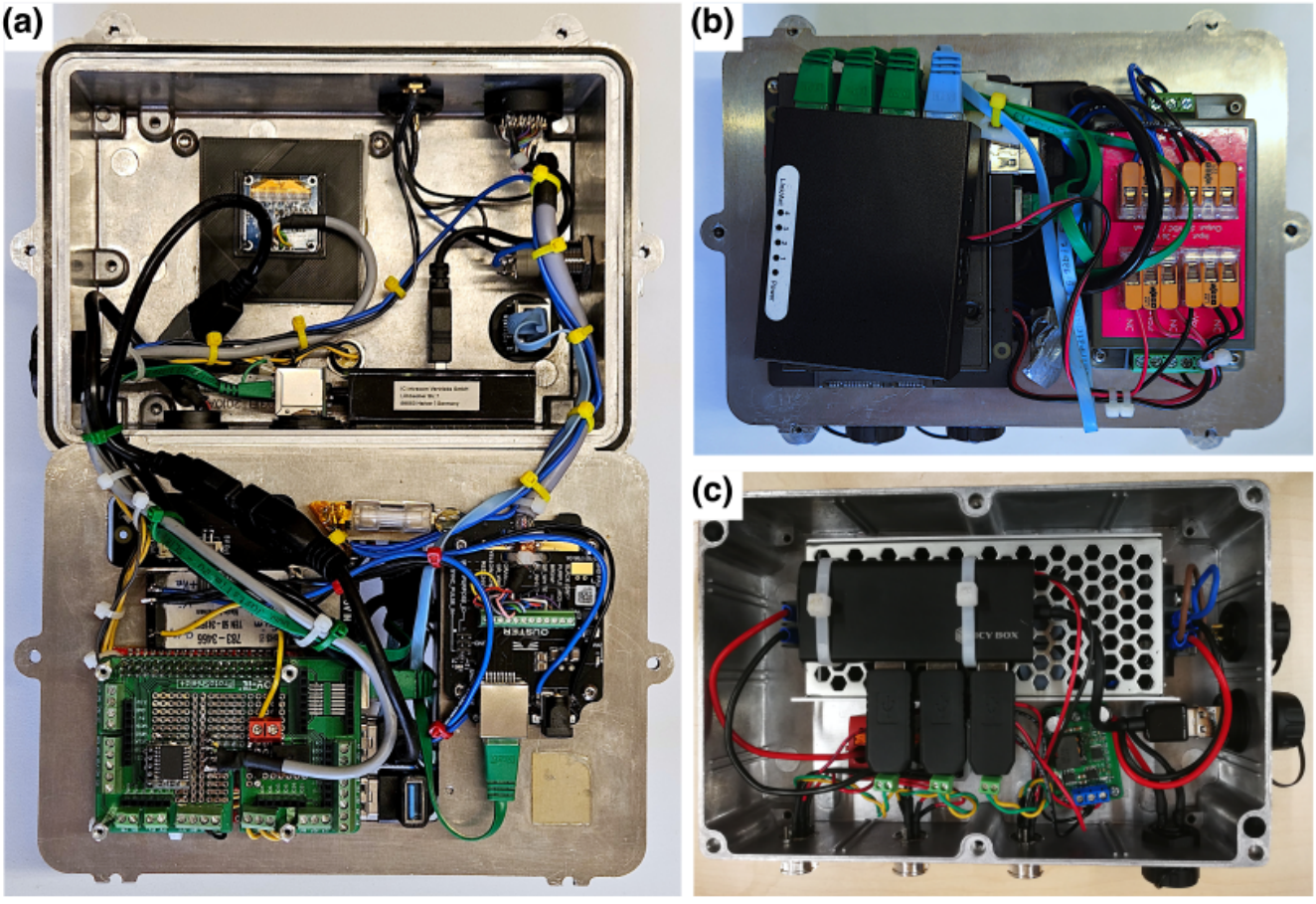

Figure 3. Internals of primary (a) and (b) and extension (c) unit. A list of the most important installed components can be found in Tab. 2.

and data transparency. Furthermore, proprietary ecosystems might impose recurring costs and restrictive licensing that can hinder the long-term sustainability of a monitoring platform. While the initial development overhead of FOSS may be higher, it should be preferred in scientific contexts to ensure platform independence, enable deep hardware integration, and uphold the principles of reproducible research.

To integrate sensors from several different manufacturers, each using different data formats and protocols, we chose the software framework ROS as a backbone for sensor communication. Originally developed at Stanford University and now maintained by Open Robotics together with an active community (Ackerman and Guizzo, 2017), ROS offers several distinct advantages over alternative frameworks (Open Robotics, 2025c). Its modular communication architecture, featuring standardized patterns (publish/subscribe, services, actions), is specifically designed for dynamic and real-time systems and is implemented through individual drivers, termed "nodes," developed in Python and C++. In contrast to classical pub/sub protocols such as MQTT, ROS provides a rich ecosystem of tools and libraries for sensor synchronization, message sending, and data

https://doi.org/10.5194/egusphere-2026-2492
Preprint. Discussion started: 10 June 2026

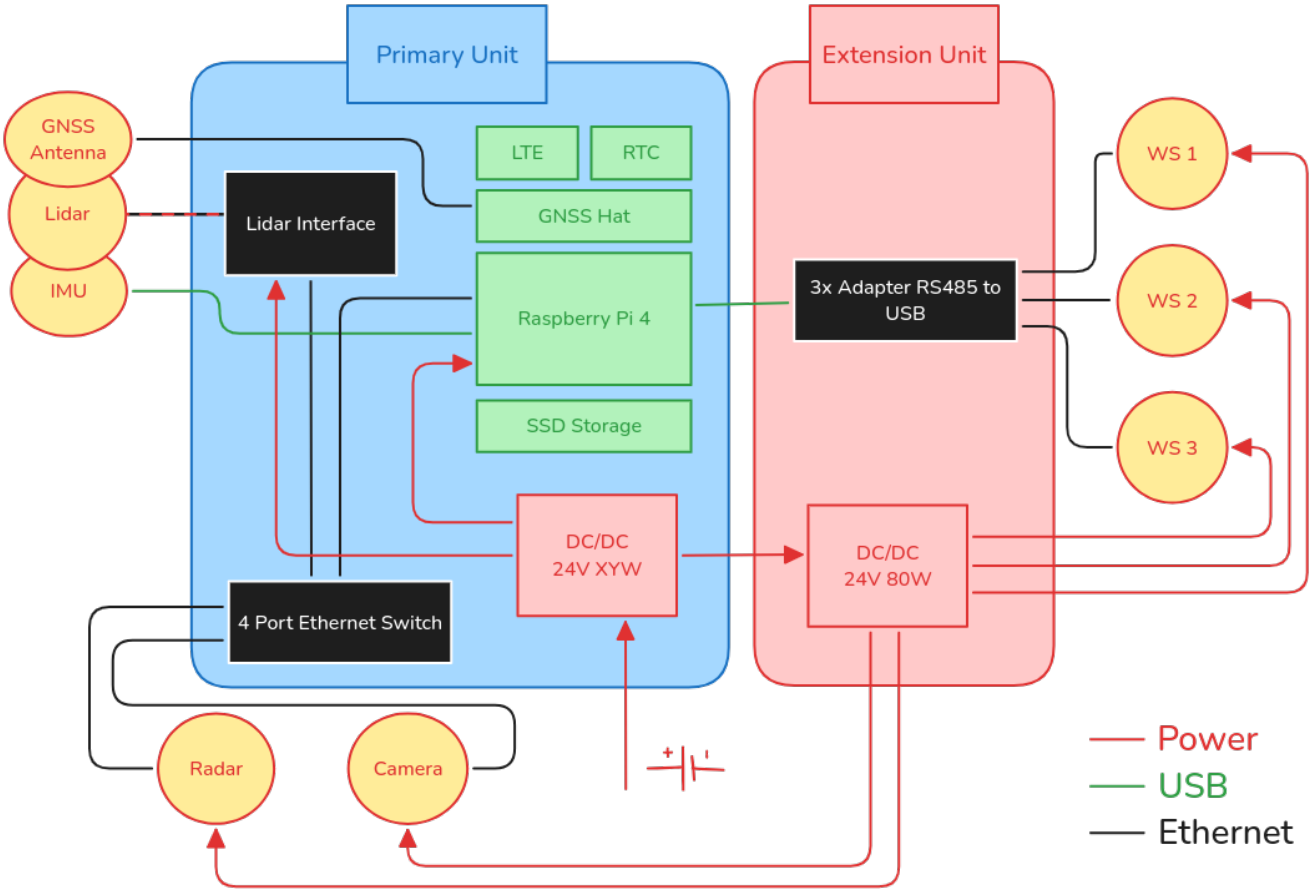

Figure 4. Block diagram of MOSEP including main components, as well as a simplified wiring overview regarding data and power.

processing, which is particularly advantageous when integrating heterogeneous sensor systems. By leveraging Data Distribution Service (DDS) as its underlying middleware, ROS decouples application logic from the communication layer and provides configurable Quality-of-Service (QoS) options (Macenski et al., 2022). Admittedly, ROS introduces some overhead in terms of performance and complexity; however, its robustness and flexibility make it a compelling choice for data collection in environmental monitoring applications. Additionally, it features standardized message types for many sensor data formats and offers numerous readily available drivers, especially for perception sensors (an incomplete list can be found in Open Robotics (2025d)). ROS is designed to cover the entire sense-plan-act cycle used in robotics, enabling autonomous systems to interact with their environment. In this project, we primarily utilize the sensing and planing stages, but ROS also facilitates the incorporation of action components. Examples include, turning on the heater of a camera housing, operating windshield wipers, or sending alerts when certain events occur.

https://doi.org/10.5194/egusphere-2026-2492
Preprint. Discussion started: 10 June 2026

Each version of ROS requires a specific release of Ubuntu. In our setup, we are using ROS2 Humble, which requires Ubuntu 22.04 LTS. To overcome this limitation and simplify development, we use a Docker-based environment that can be run on any operating system. We simplify software deployment using Docker Compose (Docker, 2026) for container orchestration, with pre-built, versioned images hosted on the GitHub Container Registry (GHCR), and a *justfile* (Rodarmor, 2026) providing shorthand commands for common operations such as starting, stopping, and updating the container. Architecture detection is handled automatically, enabling the same workflow on both x86_64 and ARM64 systems. The full set of repositories comprising the workspace is managed using vcstool (Thomas, 2026) together with a `.repos` file that pins each repository to a specific version, ensuring reproducibility. This setup streamlines development, testing, and deployment processes, thereby allowing for rapid prototyping. Nevertheless, it is not mandatory; the setup can be deployed using Docker and Git alone. The full setup, including all the code, is openly available on GitHub (https://github.com/orgs/MOLISENS-MOSEP/repositories). In conjunction with ROS, this architecture ensures not only cohesive system operation, capable of being initiated from a single launch file per application, but also the simplicity of operating individual components in isolation. For field usability, the primary unit features a straightforward interface with a three-button menu and display, and LTE support is enabling remote internet access.

For reliable measurements, our system employs three complementary time sources. GNSS, being the most accurate, is prioritized over internet timeservers; if neither is available, an onboard Real-Time Clock (RTC) with its own battery provides high-precision timestamps over extended periods. Additionally, time synchronization between the primary unit and the sensors is achieved via the network protocol called Precision Time Protocol (PTP), implemented using the linuxptp software package (Linux PTP, 2024). Although the Raspberry Pi 4 supports only software-based PTP (yielding microsecond accuracy) due to the absence of hardware support, the newer CM4 and Pi 5 models include hardware PTP (providing nanosecond accuracy), which may be beneficial for future setups. However, since extremely high-accuracy timestamps are typically less critical for environmental monitoring applications, the accuracy of the Raspberry Pi 4 was considered sufficient for the demonstration setup and use cases.

The sensor data are recorded by the ROS framework into a 'mcap' database file commonly called 'ROS bag file'. It contains all the sensor data and metadata such as the position, orientation and topology of sensors via base coordinates and transformation matrices (Fig. 5). Additionally, it comes with a unified and synchronous timeline (sensors can have different timestamps, but are synchronized). While the standard ROS PointCloud2 format can be recorded directly, we capture raw Ouster lidar data to maximize storage efficiency. Although this necessitates post-processing conversion, the raw format is approximately six times more storage efficient; for example, an hour of 10 Hz dual-return OS1 lidar data set to a spatial resolution of $1024 * 64$ points recorded in raw format results in a bag file size of 36 GB, whereas the equivalent PointCloud2 file requires 211 GB.

For streamlined data analysis, we developed a Python data pipeline (https://github.com/MOLISENS-MOSEP/analysis.moseplib) that enables the performant processing of sensor data streams and the extraction of individual measurements, known in ROS as topics. Each topic, identified by a unique hierarchical name, possesses a specific message type, which is either a standard interface or a custom definition (Open Robotics, 2025e). The dimensionality of these streams dictates the resulting data format for each timestep: 1D for single-value scalars (e.g., WS data), 2D for arrays (e.g., camera imagery), and 3D for spatial point clouds (e.g., lidar and radar).

https://doi.org/10.5194/egusphere-2026-2492
Preprint. Discussion started: 10 June 2026

We process ROS bag files by extracting time-series data and point clouds using dedicated Python libraries (Fig. 7). For 1D and 2D data, we utilize the *rosbags* library to deserialize the *mcap* database format (Ternaris UG, 2025). Depending on dimensionality, these topics are converted into the standard Python data formats, namely *pandas* Series (1D) or *pandas* DataFrames (2D).

For 3D point cloud data, we employ the *pointcloudset* library (Goelles et al., 2021), which is built upon *pandas* and *dask*. This package simplifies the handling and analysis of complex 4D datasets through its *Dataset* and *PointCloud* classes, offering efficient aggregation functions (Fig. 6), lazy loading capabilities, and visualization options. With this package, it is straightforward to apply spatial or temporal aggregations, analyze distributions, or compute statistics on individual point clouds or entire time series. As ROS inherently synchronizes time across sensors, additional alignment is generally unnecessary. Metadata, such as start time, duration, and topic details, can also be extracted directly from the ROS bag files to facilitate structured analysis. Ultimately, the pipeline enables to convert the ROS database files into standard Python data types, simplifying subsequent analyses and the derivation of scientific insights.

Additionally, ROS bag files can be inspected using the ROS tool rviz or 3rd party software like *Lichtblick* that make it simple and fast to browse through a recording and visualize sensor topics collectively, in a media player-like format.

2.4 Remote control and continuous monitoring

For on-site measurement control, the system interface is accessible via SSH from any networked computer. To enable remote monitoring and control, a VPN was integrated into the platform, allowing data to be manually transferred via SFTP or automatically synchronized with a server. For complex operational workflows, a dedicated ROS node can be implemented to automate recordings, manage sensor power states, and send system notifications regarding events such as low disk space or critical temperatures. To illustrate how such a routine is implemented, a ROS node was developed as part of a long-term monitoring setup described below. This node continuously monitors sensor data and triggers measurements upon detecting rainfall. Rather than manual operation, this node executes a logic-driven cycle by subscribing to the precipitation topic from the Lufft WS100 radar. When the precipitation rate exceeds $0\,\mathrm{mm}$ for a specified duration, the node first transitions the lidar from standby to active mode and then initiates a recording. Once precipitation remains at $0\,\mathrm{mm}$ for more than one minute, the node terminates the recording, metadata is saved, and the lidar is returned to standby mode. This routine can serve as a blueprint for adapting the platform to diverse, event-driven environmental triggers (https://github.com/MOLISENS-MOSEP/tools.met_monitoring).

3 Applications in geosciences as a complement to the automotive industry

For us, MOSEP, and application specific derivatives of it, evolved to a universal measurement platform and we belive it to be a generally usefull tool in geosciences. The low cost of components and comparably low cost of sensors make it possible to setup monitorings more easiely with less financial risk included. As recordings can be triggered once a day or 10 times per second, which makes it flexible enough for many monitoring or mapping usecases. From the gathered two- and three-dimensional data, several derived products can be calculated, such as volumes, surface change, relative reflectivity changes, and material

https://doi.org/10.5194/egusphere-2026-2492
Preprint. Discussion started: 10 June 2026

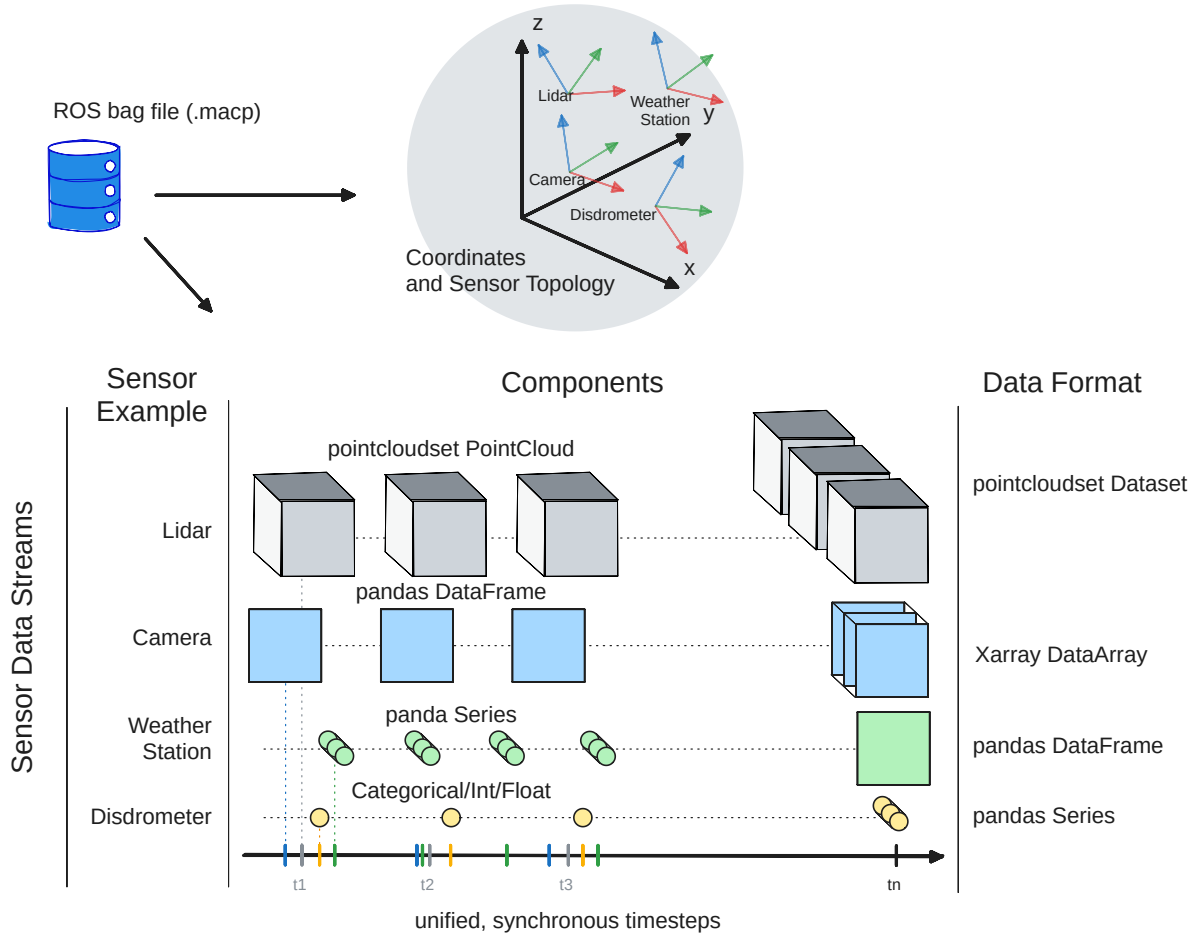

Figure 5. Contents of the 'ROS bag file' recorded by the MOSEP platform. Next to the base coordinates and transformation matrices for all sensors, sensor data streams are saved time synchronously as ROS topics. Topics are extracted as different Python data types depending on the dimensionality of the data.

https://doi.org/10.5194/egusphere-2026-2492
Preprint. Discussion started: 10 June 2026

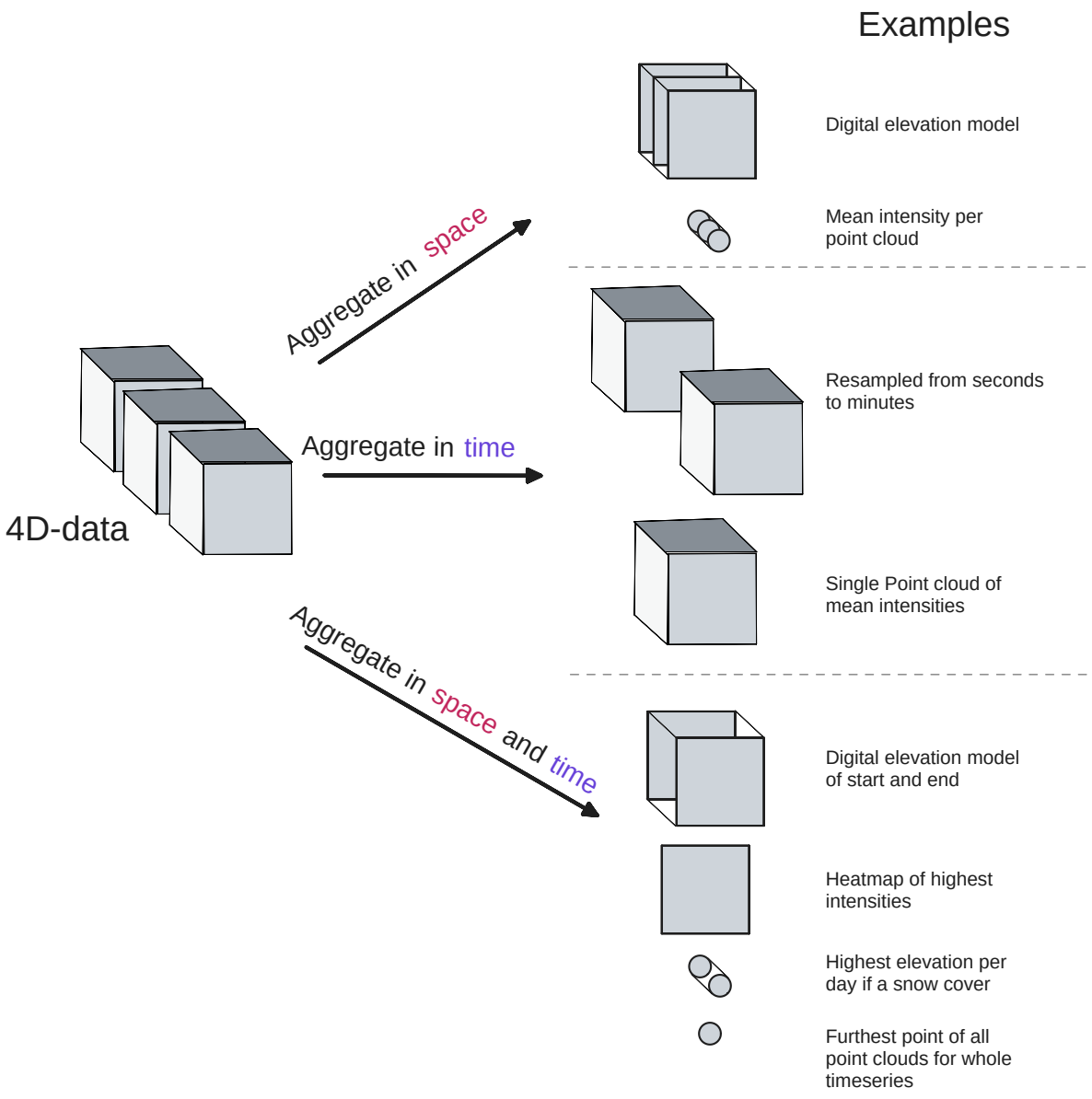

Figure 6. Possible aggregation steps in space and time that can be applied to 4D data (3 dimensions in space and one in time) with an example for each one.

https://doi.org/10.5194/egusphere-2026-2492
Preprint. Discussion started: 10 June 2026

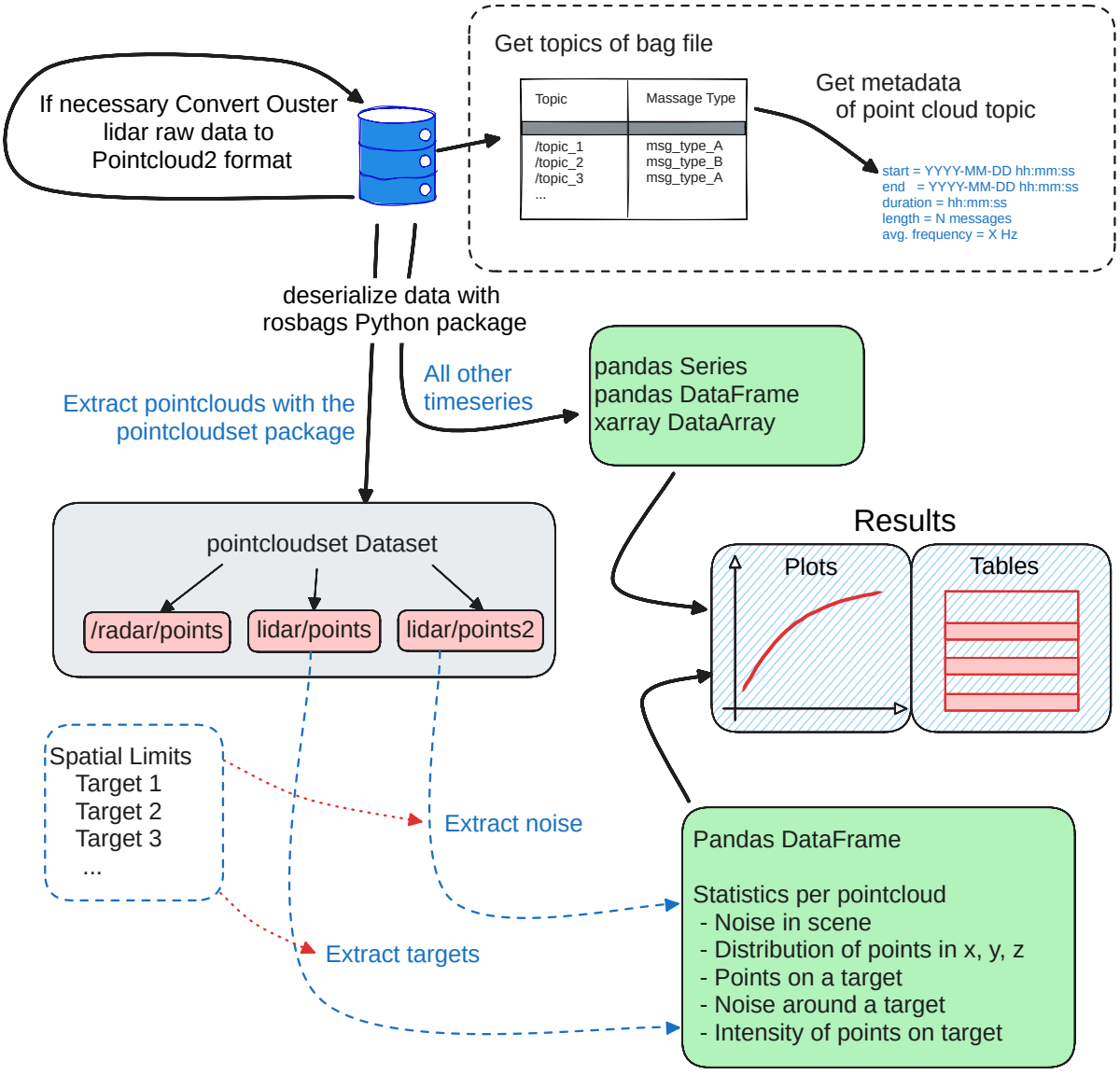

Figure 7. Data analysis workflow in Python. Depicted are the processing steps for data analysis of sensor data recorded by MOSEP. ROS topics are deserialized to either common pandas or xarray data types or in the case of point clouds to a *pointcloudset* Dataset. From there aggregation and resampling techniques can be used to extract relevant infromation.

https://doi.org/10.5194/egusphere-2026-2492
Preprint. Discussion started: 10 June 2026

classification. These products are especially usefull when investigating e.g. mass movements such as snow avalanches or rockslides, erosion monitorig or snow distribution. The true benefit of the platform emerges in a multi-sensor configuration. The inherent time-synchronous operation allows different aspects of the environment to be investigated simultaneously. For instance, a coastal mapping campaign by boat could combine lidar and sonar. Similarly, for snow monitoring, a lidar could be paired with a weather station and a camera to obtain detailed information about meteorological conditions during snow deposition.

To illustrate the versatility of MOSEP, we present two concrete applications in which the platform has been successfully employed. The first application utilizes the complete MOSEP setup, including lidar, camera, and radar, at a vehicle test track near Linz, Austria. This facility features a dedicated rain track designed to investigate how varying rain intensities affect sensor perception distance and data quality. In the second application, we employed MOSEP to evaluate its capability for iceberg detection using lidar, initially in a static configuration from shore, and subsequently aboard a vessel navigating Sermilik Fjord in East Greenland.

3.0.1 MOSEP in artificial rain

As part of a measurement campaign conducted in October 2023, we tested MOSEP at the Digitrans vehicle test track in St. Valentin, Austria (DigiTrans GmbH, 2025) during a measurement campaign by the Linz Center of Mechatronics (Reckenzaun et al., 2024). A newly constructed outdoor rain facility, approximately $80\,\mathrm{m}$ long, had recently been added to the test track (Fig. 8). The primary objective of the campaign was to evaluate the performance of different perception sensors under heavy rainfall conditions. To achieve this, the MOSEP setup, equipped with lidar, radar, and camera, was positioned just outside the rain-affected area, oriented towards an approaching vehicle. The Automatic Weather Stations (AWSs) in turn were positioned inside the rain-affect area approximately $7\,\mathrm{m}$ from the rest. During the measurement campaign, we recorded a total of 53 ROS bag files covering different rain rates (0, 30, and $100\,\mathrm{mm/h}$) and varying speeds of the approaching vehicle ($0-70\,\mathrm{km/h}$) (Gaisberger and Schlager, 2023). Although rainfall rates were simultaneously recorded using a WS100 sensor, these data proved unusable due to interference from the steel structure of the rain facility, which disrupted the upward facing radar-based precipitation measurements. Fig. 9 provides a comparison of three selected tests under different rainfall conditions. The left column displays point clouds from a single time frame, extracted using the previously introduced Python pipeline. The first lidar return is color-coded according to the intensity of the returned signal. The second lidar return and radar detections are shown in solid magenta and black, respectively. The right column presents the corresponding camera image captured from the same perspective as the lidar and radar sensors. The concentric circles on the ground clearly illustrate the impact of rainfall: the area wetted by sprinklers is particularly evident under the $30\,\mathrm{mm/h}$ rain condition. Other differences between conditions are more subtle. Notably, single frame analysis reveals very few false-positive detections (noise) caused by rain within the lidar data, and intensity degradation in the lidar returns from the vehicle is surprisingly limited. Radar reliably detects both the car and a truck in the background; however, the number of false-positive radar detections noticeably increases with rainfall intensity, as is evident by the prominent false-positive cluster appearing at $100\,\mathrm{mm/h}$ rain. The time synchronously captured camera images proved highly valuable for interpreting the point clouds, demonstrating their significance as a complementary

https://doi.org/10.5194/egusphere-2026-2492
Preprint. Discussion started: 10 June 2026

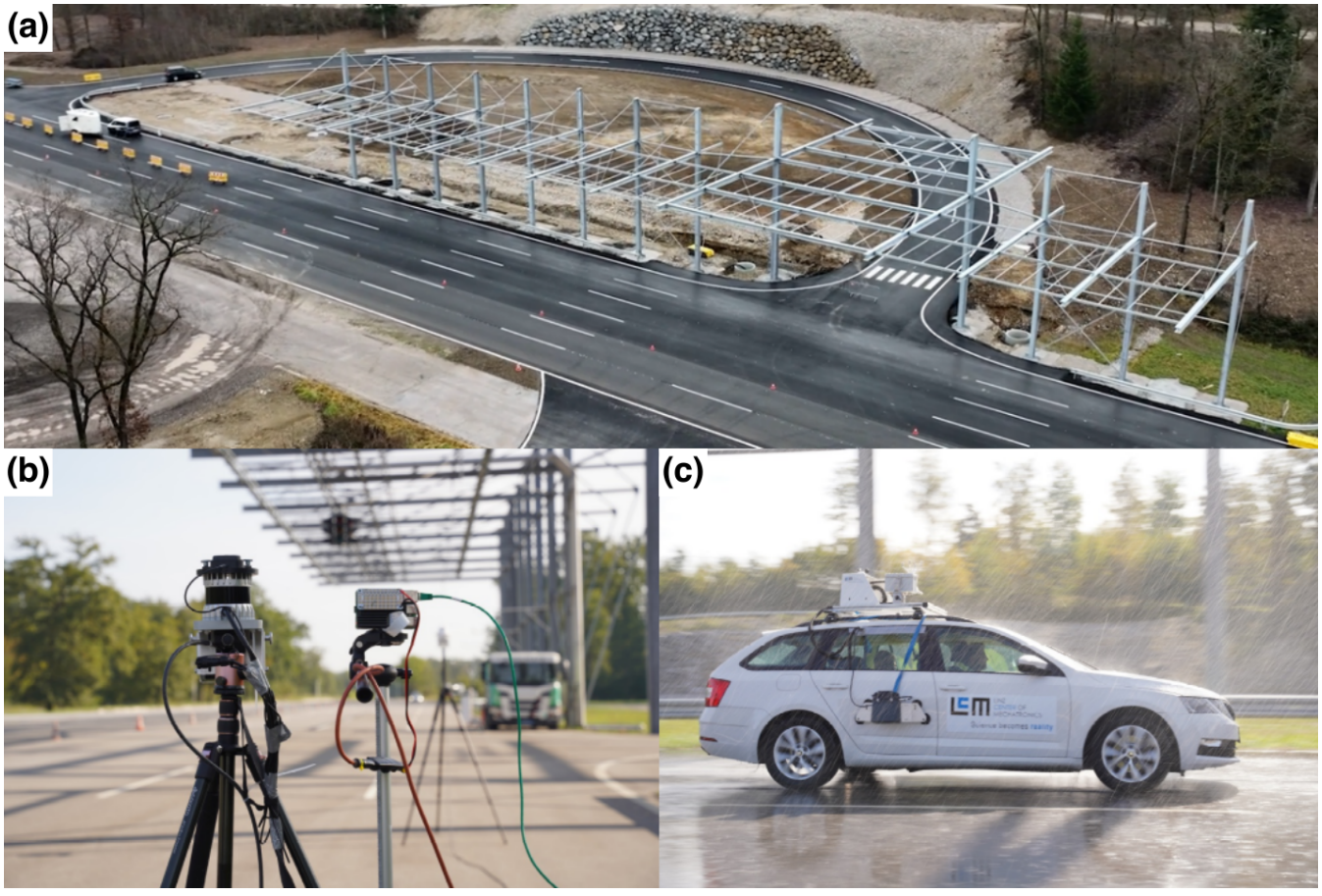

Figure 8. (a) The Digitrans test track with a rain simulator; (b) the MOSEP measurement setup with lidar and radar on the left tripod and the camera (without housing) on the right tripod; and (c) the observed vehicle.

component of the sensor suite. Nevertheless, the presented analysis serves primarily to illustrate the capabilities of MOSEP, and a more in-depth investigation is required to fully characterize the impacts of adverse weather on perception sensors.

3.0.2 MOSEP for observing icebergs and whales in Greenland

During a field campaign at the joint Danish-Austrian research station in Sermilik Fjord, East Greenland, we evaluated MOSEP across various environmental scenarios. One experiment involved the observation of icebergs using lidar, as illustrated in Fig. 10. The resulting scan was generated by walking along the shoreline while continuously recording lidar, GNSS, and IMU data, subsequently registering individual point clouds into a unified map using SLAM. The OS1 lidar was able to detect medium-sized icebergs at distances of up to 80 m from the shore. Since snow and ice exhibit high reflectivity in the near-infrared spectrum, whereas water strongly absorbs radiation at these wavelengths (McManamon, 2019), the icebergs are clearly discernible within the lidar data. Despite the high turbidity characteristic of glacial fjords-often containing significant concentrations of

https://doi.org/10.5194/egusphere-2026-2492
Preprint. Discussion started: 10 June 2026

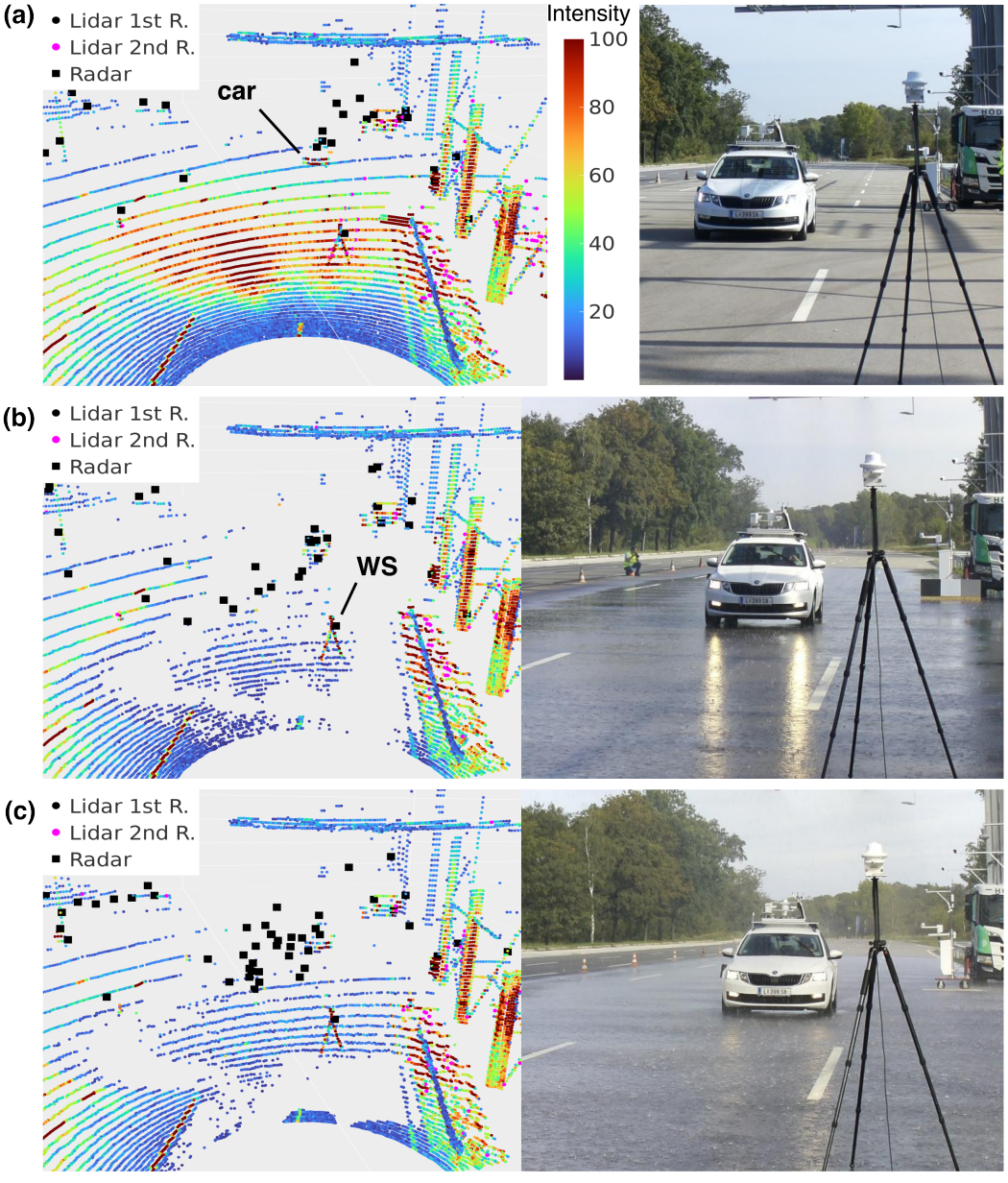

Figure 9. Comparison of a reference measurement without artificial rain (a) and two measurements with 30 mm/h (b) and $100\,\mathrm{mm/h}$ (c) with point clouds from lidar and radar in the left column and the corresponding camera images in the right column. Round points are from the lidar with the ones colored from blue to red depicting intensity values of the strongest lidar return. Purple points correspond to the second strongest lidar return. Radar measurements are shown as black squares.

https://doi.org/10.5194/egusphere-2026-2492
Preprint. Discussion started: 10 June 2026

suspended sediment known as 'glacier milk'-the OS1 lidar demonstrated limited subsurface penetration. While no returns were received from below the water surface at shallow (near-grazing) angles, at steeper incidence angles-when objects in the water were sufficiently close, the lidar was seeminmgly capable of penetrating below the surface. The blue points in panels a) and b) indicate returns from below the waterline, at an apparent depth of approximately $3\,\mathrm{m}$. It is important to note that these values may represent reflections from surfaces above the water, a possibility that is especially true for deeper points as water is highly absorbing in the infrared spectrum. If returns are genuinely from below the surface, the measured distances represent the optical path length; to derive the true depth, a correction for the refractive index of water ($n \approx 1.33$) must be applied as well as the lower speed of light in water must be taken into account. At shallower incidence angles (greater distances from the lidar), the absence of returns is attributed to specular reflection, where the smooth water surface reflects the laser energy away from the sensor rather than backscattering it to the receiver (Millard and Seaver, 1990).

In a subsequent measurement conducted aboard a small ship, we unexpectedly recorded a pod of humpback whales. Similar to icebergs, whales stand out clearly against the water, as illustrated in Fig. 11. Additionally, the whales' blow clouds from surfacing are distinctly visible above them. To compensate for the majority of the movement of the boat during data acquisition, the resulting point clouds were linearly shifted along the x-axis, causing the boat itself to appear stretched in the processed data.

4 Discussion and outlook

In this work, we introduced MOSEP, a modular, open-source platform designed to integrate automotive perception sensors with general environmental sensors for scientific monitoring. Addressing the need for flexible, robust, and cost-effective solutions, MOSEP successfully interfaces advanced autonomous vehicle technologies with practical field applications. The platform combines low-cost automotive lidar, radar, camera, GNSS, IMU, and meteorological sensors into a compact, field-ready unit. It demonstrates the feasibility of continuous, multi-modal sensing and enables time-synchronized data capture. Field trials in diverse conditions, from controlled rain simulations to Arctic deployments, validated its reliability. By utilizing FOSS with ROS2 and a containerized environment, we provide a scalable and accessible solution for researchers in geosciences, ecology, and related fields. MOSEP's high temporal resolution and mobility allow it to capture rapid changes and small-scale phenomena often missed by coarse satellite observations, providing a vital "middle ground" between sparse in-situ measurements and broad remote sensing.

The core contributions of MOSEP lie in its fully integrated hardware suite and complementary software architecture. On the hardware side, we designed a modular, battery-powered platform that brings together six different sensor modalities in a single mobile unit. All sensors share a common $24\,\mathrm{V}$ power supply and are housed in a weatherproof enclosure, making the system compact and easily transportable. This integration overcomes the lack of "plug-and-play" availability in raw perception sensors by providing a unified wiring and mounting framework. The result is an adaptable setup where components can be added or exchanged with minimal effort, giving researchers the freedom to tailor the sensor suite to a specific projects needs. On the software side, we implemented a ROS2-based middleware that handles real-time sensor data streaming, time synchronization,

https://doi.org/10.5194/egusphere-2026-2492
Preprint. Discussion started: 10 June 2026

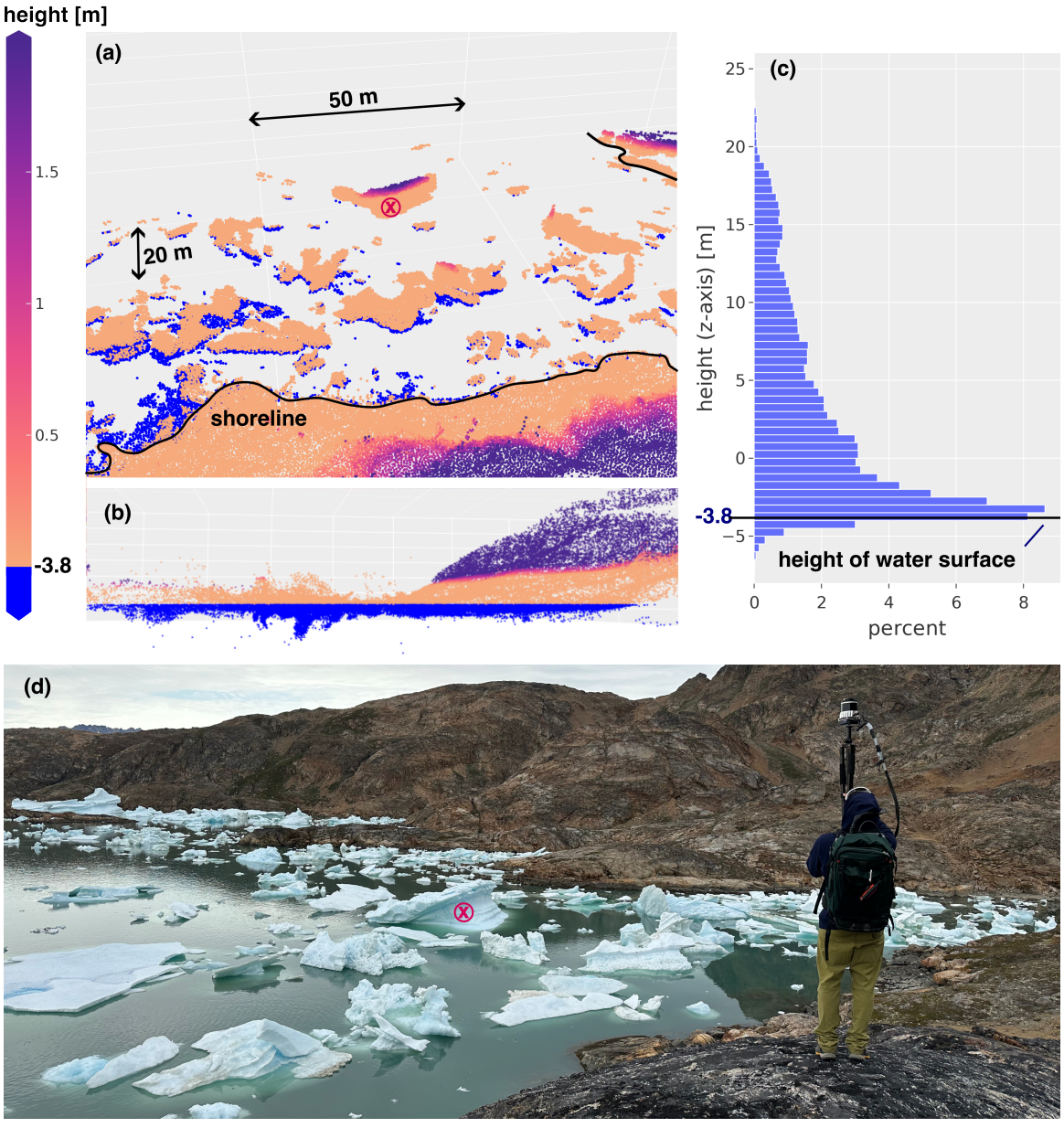

Figure 10. Iceberg monitoring with MOSEP in front of Sermilik research station in Sermilik fjord, East Greenland. Panels (a) (oblique view) and (b) (side view) show the SLAM generated lidar point cloud from the recording. The rocky shoreline as well as floating icebergs are very well visible in contrast to water. For steep enough incidence angles submerged parts below $-3.8\,\mathrm{m}$ are recognized by the lidar (highlighted in blue). The height distribution of points in (c) reveal the approximate location of the waterline. For comparison one icebearg is marked with a red X in (a) and (d) which was located around $52\,\mathrm{m}$ from the shore.

https://doi.org/10.5194/egusphere-2026-2492
Preprint. Discussion started: 10 June 2026

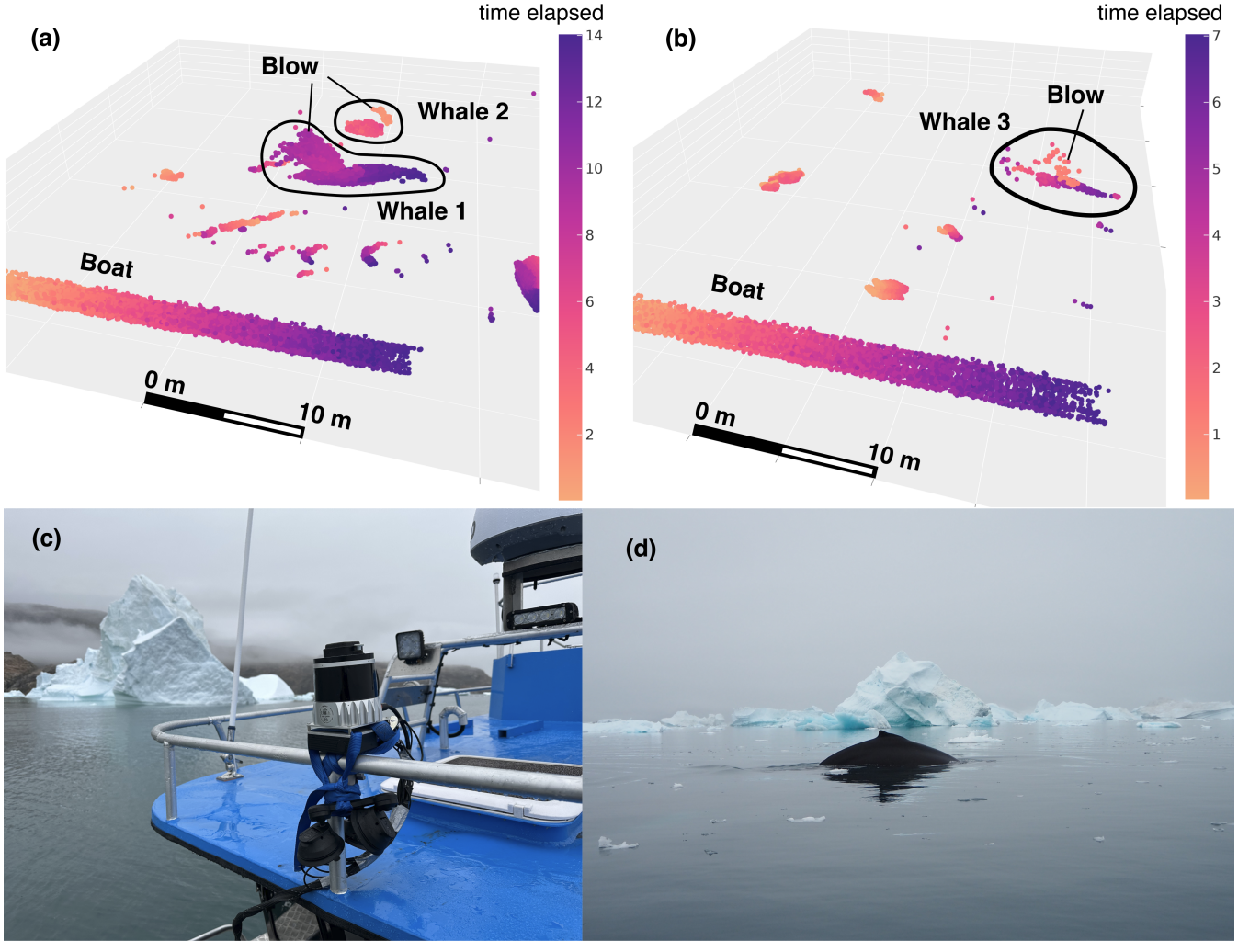

Figure 11. Lidar data of icebergs from a boat (a) and (b). The lidar was mounted to the railing at the top front of the boat (c). During the campaign a pod of humpback whales showed up now also visible in the data (d). Points are colored by time (seconds from the first frame).

https://doi.org/10.5194/egusphere-2026-2492
Preprint. Discussion started: 10 June 2026

and logging. Time-synchronous recording into a single database significantly simplifies subsequent data analysis and fusion. By containerizing the stack using Docker Compose, we ensure the entire codebase is openly available and easily replicable on any Linux system. A key contribution of MOSEP to the geoscience community is not only the integration of additional perception and meteorological sensors into a single synchronized platform, but also the provision of a dedicated analysis pipeline and the structured publication of both hardware and software, enabling reproducible reuse and adaptation in new monitoring applications.

The use of automotive lidar and radar offers an affordable alternative to high-end instruments like TLS, trading some absolute accuracy for greater field versatility and higher temporal resolution. This approach aligns with a broader trend toward accessible, cost-effective, open-source solutions. Here, we particularly focus on extending advanced multi-sensor monitoring into challenging domains such as alpine and polar research.

In field tests, we have demonstrated MOSEP's capabilities under diverse artificial and real-world conditions. In rain simulation tests, the Ouster lidar proved remarkably resilient; even at high intensities, point clouds showed almost no spurious returns from raindrops, and only a slight reduction in return signal intensity from the target. The radar continued to detect the test vehicle reliably at all rain levels; while higher rain rates introduced some false-positive radar detections. Importantly, the co-located camera provided visual context to interpret the lidar and radar data, illustrating the value of multi-sensor cross-validation in challenging conditions. An in depth analysis of the findings will be part of a future paper.

Additional deployments in East Greenland illustrated the system's potential for monitoring in harsh conditions such as cryospheric or marine environments. Icebergs were sharply distinguished against the water due to the high reflectivity of snow and ice in the lidar's near-infrared spectrum. In the Greenland application, we achieved reliable lidar detection of medium-sized icebergs at ranges of up to $80\,\mathrm{m}$ with cm-level precision. While the Ouster OS1 sensor used for this test cost approximately $10,000\,\mathrm{EUR}$ at the time, comparable or better performance can now be achieved with newer sensors, such as the Livox Avia, for around $1,500\,\mathrm{EUR}$ (Livox, 2026). Combined with the low platform cost of under $2,000\,\mathrm{EUR}$, this demonstrates that a highly capable system can be built for a fraction of the cost of traditional terrestrial laser scanners, while also offering greater deployment flexibility and integration options. Notably, the system serendipitously detected a pod of humpback whales during a fjord transit. The whales appeared clearly in the 3D point clouds, and even the ephemeral spray from their blowholes was captured. This unplanned wildlife observation underscores the broad scope of MOSEP: the same setup used for ice mapping was able to track large marine animals in real time.

The ability to capture environmental changes at sub-second intervals (10-20 Hz) opens new avenues for studying rapid dynamics such as snowfall evolution, iceberg decay, or animal interactions. The mobility and affordability of such a system make it a valuable tool for natural hazard monitoring and prevention, enabling frequent, high-resolution data collection for applications like debris flow analysis, avalanche safety, and geological process monitoring (Aaron et al., 2023; Goelles et al., 2025; Garcia-Sellés et al., 2023; Deems et al., 2013). However, a major challenge remains the "black box" nature of many industrial sensors, which can make in depth anlysis problematic. For expample both lidar and radar perform significant internal signal processing. This complicates calibration and data interpretation and makes it difficult to derive physical properties, such as precise lidar intensity values. Additionally, while centimeter-level precision is sufficient for many applications, the

https://doi.org/10.5194/egusphere-2026-2492
Preprint. Discussion started: 10 June 2026

limited range of automotive sensors remains one of the greatest challenges for us. State-of-the art automotive lidar systems, such as the Livox Avia (https://www.livoxtech.com/avia), provide a maximum range of up to $450\,\mathrm{m}$ acoording to manufacturer specifications. From our experience, realistic maximum ranges vary between $250\text{-}420\,\mathrm{m}$ depending on target reflectivity and incidence angle (Goelles et al., 2025). The maximum range of automotive lidar sensors might increase significantly with technologies such as VCSEL (Vertical-Cavity Surface-Emitting Laser) trasmitter, SPAD (Single-photon avalanche diode) receiver and FMCW technolgies. Operationally, MOSEP requires a certain level of technical expertise in electronics and ROS2. While we have streamlined the process with the provided software and documentation, users still need to understand ROS2, manage power and data, and perform calibrations for accurate sensor fusion. Unlike turnkey commercial systems, it demands active management of power and data: running multiple sensors at high frequency can consume a significant amount power. Field deployments must ensure a stable power supply and plan for possibly large volumes of data storage or transfer. In our tests, we mitigated this using automated triggers and offloading data periodically, but long-term autonomous operation requires careful planning. Despite these limitations, the benefits of MOSEP, particularly its flexibility and cost-effectiveness, generally outweigh the drawbacks for targeted environmental research.

5 Conclusions

The primary objective of this paper and the development of MOSEP is to provide a foundational platform that motivates the geoscience and ecology communities to leverage emerging perception sensors. By releasing the hardware designs and software under open-source licenses, we aim to lower the barrier to entry, encouraging researchers to adopt and adapt this platform for their specific monitoring requirements. We believe this open approach will accelerate innovation in environmental sensing through community-driven improvements. Planned future work includes long-term deployments in alpine regions to continuously monitor snowpack accumulation, avalanche formation, and release events (Goelles et al., 2025). A particularly interesting avenue of research is the development of precipitation rate inference from lidar noise patterns. By using these patterns as a proxy for precipitation intensity, MOSEP could complement or calibrate traditional rain sensors by providing high-resolution spatial data on rainfall within the lidar's field of view. Additionally, we intend to explore the possibilities of enhanced sensor fusion algorithms offering many research opportunities, where the addition of further modalities such as sonar, acoustic, or thermal sensors could provide a more comprehensive environmental picture. By continuing these efforts, we hope to foster a broader adoption of automotive-derived perception sensors within environmental science, enhancing the capacity to observe, understand, and respond to environmental processes. Ultimately, MOSEP represents a modest but meaningful step toward more accessible, continuous monitoring in challenging environments, complementing traditional observation networks and fostering cross-disciplinary innovation.

Code availability. All the mentioned code is fully available under MIT License at https://github.com/orgs/MOLISENS-MOSEP/repositories

https://doi.org/10.5194/egusphere-2026-2492
Preprint. Discussion started: 10 June 2026

Data availability. An example dataset from the Digitrans test track including lidar, camera, radar and weather staion data are available at https://zenodo.org/uploads/19353314

Author contributions. Conceptualization, CG and SM; methodology, CG, SM and TG; software, CG and MS; writing-original draft preparation, CG; writing-review and editing, CG, WS, SM, BS, TG, MS and SG; visualization, CG; supervision, SM and WS; project administration, CG and SM; funding acquisition, SM. All authors have read and agreed to the published version of the manuscript.

Competing interests. The authors declare that they have no conflict of interest. The funders had no role in the design of the study; in the collection, analyses, or interpretation of data; in the writing of the manuscript, or in the decision to publish the results.

Acknowledgements. This work was partially financed by Virtual Vehicle Research GmbH, a COMET K2 Competence Centers for Excellent Technologies funded by the Austrian Federal Ministry for Climate Action (BMK), the Austrian Federal Ministry for Labor and Economy (BMAW), the Province of Styria (Dept. 12) and the Styrian Business Promotion Agency (SFG). The Austrian Research Promotion Agency (FFG) has been authorized for the programme management. They would furthermore like to express their thanks to their supporting industrial and scientific project partners, namely Infineon Technologies Austria AG, Ing. h. c. F. Porsche AG, Volkswagen AG, aiMotive Kft, Joanneum Research, University of Klagenfurt,Technical University Graz and University of Graz. The research was also partially carried out within the framework of the project testEPS. The EUREKA project testEPS is funded by the Austrian Federal Ministry of climate action, environment, mobility, innovation and Technology (BMK) through the program "Mobilität der Zukunft (MdZ)" - 16. Ausschreibung Automatisierte Mobilität (EUREKA 2020) and by the Hungarian Federal Ministry of Transport, Innovation and Technology, Hungarian Funding Agency. Additionally, this work was partially funded by the “Austrian Space Application Programme” of the FFG within the project RSnowAUT. We would like to thank the Linz Center of Mechatronics for giving us the opportunity to participate in the measurement campaign at the Digitrans test track. Lastly, we would like to thank the local community of Tasiilaq in East Greenland for their invaluable local knowledge and support of our work at the Sermilik Research Station.

During the preparation of this manuscript, the authors utilized AI assistance (Gemini 2.5 Pro and Claude Sonnet 4.6) to improve text clarity, grammar, and formatting. These tools were also used to aid in software documentation and improve code reliability.

https://doi.org/10.5194/egusphere-2026-2492
Preprint. Discussion started: 10 June 2026

References

Aaron, J., Spielmann, R., McArdell, B. W., and Graf, C.: High-Frequency 3D LiDAR Measurements of a Debris Flow: A Novel Method to Investigate the Dynamics of Full-Scale Events in the Field, Geophysical Research Letters, 50, e2022GL102 373, https://doi.org/10.1029/2022GL102373, 2023.

Ackerman, E. and Guizzo, E.: Wizards of ROS: Willow Garage and the Making of the Robot Operating System - IEEE Spectrum, IEEE Spectrum, 2017.

Aerial Precision: AP-LiDAR-One Gen II, https://www.aerial-precision.com/pages/ap-lidar-one-gen-ii, product Page, 2025.

Chiang, K.-W., Tsai, G.-J., Li, Y.-H., and El-Sheimy, N.: Development of LiDAR-Based UAV System for Environment Reconstruction, IEEE Geoscience and Remote Sensing Letters, 14, 1790–1794, https://doi.org/10.1109/LGRS.2017.2736013, 2017.

Christiansen, M. P., Laursen, M. S., Jørgensen, R. N., Skovsen, S., and Gislum, R.: Designing and Testing a UAV Mapping System for Agricultural Field Surveying, Sensors, 17, 2703, https://doi.org/10.3390/s17122703, 2017.

Deems, J. S., Painter, T. H., and Finnegan, D. C.: Lidar Measurement of Snow Depth: A Review, Journal of Glaciology, 59, 467–479, https://doi.org/10.3189/2013JoG12J154, 2013.

Dharmadasa, V., Kinnard, C., and Baraër, M.: An Accuracy Assessment of Snow Depth Measurements in Agro-Forested Environments by UAV Lidar, Remote Sensing, 14, 1649, https://doi.org/10.3390/rs14071649, 2022.

DigiTrans GmbH: Outdoor Rain Plant, https://www.digitrans.expert/en/outdoor-rain-plant/, 2025.

Dikic, B., Goelles, T., Gaisberger, C., Schlager, B., Muckenhuber, S., Batista, P., Keuschnig, M., and Schratter, M.: Lidar-Based Snow Monitoring from Aerial Lifts: Gondola Deployment in the Austrian Alps, Journal of Glaciology, 72, e12, https://doi.org/10.1017/jog.2025.10105, 2026.

Docker: Docker/Compose, https://github.com/docker/compose, 2026.

Filhol, S., Perret, A., Girod, L., Sutter, G., Schuler, T. V., and Burkhart, J. F.: Time-Lapse Photogrammetry of Distributed Snow Depth During Snowmelt, Water Resources Research, 55, 7916–7926, https://doi.org/10.1029/2018WR024530, 2019.

Foxglove: MCAP - Open Source Container File Format for Multimodal Log Data, https://mcap.dev/, 2025.

Gaisberger, C.: ROS 2 Driver for Luff-UMB Weather Sensor, https://github.com/MOLISENS-MOSEP/drivers.lufft_weather_station, 2025.

Gaisberger, C. and Schlager, B.: MOSEP DigiTrans Rain Simulation Demo Dataset, https://doi.org/10.5281/zenodo.19353314, 2023.

Garcia-Sellés, O., Guinau, M., Eras, M., Montesinos, P., Ramos, M., and Ferrer, O.: Geological Monitoring Processes with Small Laser Scanners. Examples in Montserrat, Puigcercós, Croscat Volcano (Catalonia, Spain) and Analogic Models, in: 5th Virtual Geoscience Conference, Dresden, 2023.

Goelles, T., Schlager, B., Muckenhuber, S., Haas, S., and Hammer, T.: 'pointcloudset': Efficient Analysis of Large Datasets of Point Clouds Recorded Over Time, https://doi.org/10.21105/joss.03471, 2021.

Goelles, T., Hammer, T., Muckenhuber, S., Schlager, B., Abermann, J., Bauer, C., Expósito Jiménez, V. J., Schöner, W., Schratter, M., Schrei, B., and Senger, K.: MOLISENS: MObile LIdar SENsor System to Exploit the Potential of Small Industrial Lidar Devices for Geoscientific Applications, Geoscientific Instrumentation, Methods and Data Systems, 11, 247–261, https://doi.org/10.5194/gi-11-247-2022, 2022.

Goelles, T., Wallner, S., and Eckerstorfer, M.: Low Cost Lidar Monitoring for Planning and Operation of Mitigation Measures, in: Proceedings of the International Symposium on Mitigation Measures against Snow Avalanches and Other Rapid Gravity Mass Flows, Ísafjörður, Iceland, 2025.

https://doi.org/10.5194/egusphere-2026-2492
Preprint. Discussion started: 10 June 2026

Hotaling, S., Lutz, S., Dial, R. J., Anesio, A. M., Benning, L. G., Fountain, A. G., Kelley, J. L., McCutcheon, J., Skiles, S. M., Takeuchi, N., and Hamilton, T. L.: Biological Albedo Reduction on Ice Sheets, Glaciers, and Snowfields, Earth-Science Reviews, 220, 103 728, https://doi.org/10.1016/j.earscirev.2021.103728, 2021.

Hu, T., Sun, X., Su, Y., Guan, H., Sun, Q., Kelly, M., and Guo, Q.: Development and Performance Evaluation of a Very Low-Cost UAV-Lidar System for Forestry Applications, Remote Sensing, 13, 77, https://doi.org/10.3390/rs13010077, 2021.

Hyyppä, E., Kukko, A., Kaijaluoto, R., White, J. C., Wulder, M. A., Pyörälä, J., Liang, X., Yu, X., Wang, Y., Kaartinen, H., Virtanen, J.-P., and Hyyppä, J.: Accurate Derivation of Stem Curve and Volume Using Backpack Mobile Laser Scanning, ISPRS Journal of Photogrammetry and Remote Sensing, 161, 246–262, https://doi.org/10.1016/j.isprsjprs.2020.01.018, 2020.

Jacobs, J. M., Hunsaker, A. G., Sullivan, F. B., Palace, M., Burakowski, E. A., Herrick, C., and Cho, E.: Snow Depth Mapping with Unpiloted Aerial System Lidar Observations: A Case Study in Durham, New Hampshire, United States, The Cryosphere, 15, 1485–1500, https://doi.org/10.5194/tc-15-1485-2021, 2021.

Ji, W., Hao, X., Shao, D., Yang, Q., Wang, J., Li, H., and Huang, G.: A New Index for Snow/Ice/Ice-Snow Discrimination Based on BRDF Characteristic Observation Data, Journal of Geophysical Research: Atmospheres, 127, e2021JD035 742, https://doi.org/10.1029/2021JD035742, 2022.

Jokela, M., Kutila, M., and Pyykönen, P.: Testing and Validation of Automotive Point-Cloud Sensors in Adverse Weather Conditions, Applied Sciences, 9, 2341, https://doi.org/10.3390/app9112341, 2019.

King, F., Kelly, R., and Fletcher, C. G.: New Opportunities for Low-Cost LiDAR-derived Snow Depth Estimates from a Consumer Drone-Mounted Smartphone, Cold Regions Science and Technology, 207, 103 757, https://doi.org/10.1016/j.coldregions.2022.103757, 2023.

Kutila, M., Pyykönen, P., Holzhüter, H., Colomb, M., and Duthon, P.: Automotive LiDAR Performance Verification in Fog and Rain, in: 2018 21st International Conference on Intelligent Transportation Systems (ITSC), pp. 1695–1701, ISSN 2153-0017, https://doi.org/10.1109/ITSC.2018.8569624, 2018.

Linux PTP: The Linux PTP Project, https://linuxptp.sourceforge.net/, 2024.

Livox: Specs - Avia LiDAR Sensor, https://www.livoxtech.com/avia/specs, 2026.

Macenski, S., Foote, T., Gerkey, B., Lalancette, C., and Woodall, W.: Robot Operating System 2: Design, Architecture, and Uses in the Wild, Science Robotics, 7, eabm6074, https://doi.org/10.1126/scirobotics.abm6074, 2022.

McManamon, P. F.: LiDAR Technologies and Systems, SPIE Press, Bellingham, Washington, USA, ISBN 978-1-5106-2539-6, 2019.

Millard, R. C. and Seaver, G.: An Index of Refraction Algorithm for Seawater over Temperature, Pressure, Salinity, Density, and Wavelength, Deep Sea Research Part A. Oceanographic Research Papers, 37, 1909–1926, https://doi.org/10.1016/0198-0149(90)90086-B, 1990.

Open Robotics: ROS 2 Documentation - Concepts, https://docs.ros.org/en/humble/Concepts.html, 2025a.

Open Robotics: ROS 2 Documentation - Recording a Bag from a Node (Python), https://docs.ros.org/en/humble/Tutorials/Advanced/Recording-A-Bag-From-Your-Own-Node-Py.html, 2025b.

Open Robotics: ROS 2 - Version 2 of the Robot Operating System (ROS) Software Stack, https://github.com/ros2, 2025c.

Open Robotics: ROS Device Drivers, https://github.com/ros-drivers, 2025d.

Open Robotics: ros2/Common_interfaces, https://github.com/ros2/common_interfaces, 2025e.

OTT HydroMet: Lufft WS100 Radar Precipitation Sensor, https://www.lufft.com/products/precipitation-sensors-287/ws100-radar-precipitation-sensor-smart-disdrometer-2361/, datasheet, 2024a.

OTT HydroMet: Lufft WS501 UMB, https://www.lufft.com/products/compact-weather-sensors-293/ws501-umb-smart-weather-sensor-1839/, datasheet, 2024b.

https://doi.org/10.5194/egusphere-2026-2492
Preprint. Discussion started: 10 June 2026

Ouster: Digital Lidar: Realizing the Power of Moore's Law, https://ouster.com/insights/blog/digital-lidar-realizing-the-power-of-moores-law, 2024.

Ouster: OS1/OS2, https://ouster.com/downloads, datasheet, 2025.

Perks, M. T., Pitman, S. J., Bainbridge, R., Díaz-Moreno, A., and Dunning, S. A.: An Evaluation of Low-Cost Terrestrial Lidar Sensors for Assessing Hydrogeomorphic Change, Earth and Space Science, 11, e2024EA003 514, https://doi.org/10.1029/2024EA003514, 2024.

Raman, M. G., Carlos, E. F., and Sankaran, S.: Optimization and Evaluation of Sensor Angles for Precise Assessment of Architectural Traits in Peach Trees, Sensors, 22, 4619, https://doi.org/10.3390/s22124619, 2022.

Raspberry Pi: Documentation - Camera Modules, https://www.raspberrypi.com/documentation/accessories/camera.html, 2025.

Rauhala, A., Meriö, L.-J., Kuzmin, A., Korpelainen, P., Ala-aho, P., Kumpula, T., Kløve, B., and Marttila, H.: Measuring the Spatiotemporal Variability in Snow Depth in Subarctic Environments Using UASs – Part 1: Measurements, Processing, and Accuracy Assessment, The Cryosphere, 17, 4343–4362, https://doi.org/10.5194/tc-17-4343-2023, 2023.

Reckenzaun, J., Rott, R., Nikolić, O., Innerwinkler, P., Kirchengast, M., Ritter, D. J., Solmaz, S., Ladstätter, S., Luley, P., Toth, B., Hee, A. M., Hörmann, L., Pötsch, A., Rothacher, M., Rövid, A., Vincze, Z., and Csonthó, M.: Transnational Testing, Operation and Certification of Automated Driving Systems – Building Bricks for the NATM Multi-Pillar Framework, in: 2024 IEEE International Automated Vehicle Validation Conference (IAVVC), pp. 1–7, https://doi.org/10.1109/IAVVC63304.2024.10786414, 2024.

Renette, C., Thorson, S., Olvmo, M., Holmer, B., and Reese, H.: Multitemporal UAV LiDAR Detects Seasonal Heave and Subsidence on Palsas, in: EGU24, Copernicus Meetings, https://doi.org/10.5194/egusphere-egu24-630, 2024.

Rodarmor, C.: Casey/Just, 2026.

RS Components: 3 Pole Connector IP68, https://docs.rs-online.com/6827/A700000009053776.pdf, datasheet, 2025.

Ruttner-Jansen, P., Voordendag, A., Hartmann, T., Glaus, J., Wieser, A., and Bühler, Y.: Monitoring Snow Depth Variations in an Avalanche Release Area Using Low Cost LiDAR and Optical Sensors, EGUsphere, pp. 1–20, https://doi.org/10.5194/egusphere-2024-744, 2024.

SATLAB: Cygnus, https://www.satlab.com.se/product/cygnus-handheld-slam-scanner/, 2025.

Smartmicro: UMRR-11 Type 132, https://www.smartmicro.com/fileadmin/media/Downloads/Automotive_Radar/Sensor_Data_Sheets_76-81GHz/UMRR-11_Type_132_Automotive_Data_Sheet.pdf, datasheet, 2021.

Štroner, M., Urban, R., Křemen, T., and Braun, J.: UAV DTM Acquisition in a Forested Area – Comparison of Low-Cost Photogrammetry (DJI Zenmuse P1) and LiDAR Solutions (DJI Zenmuse L1), European Journal of Remote Sensing, 56, 2179 942, https://doi.org/10.1080/22797254.2023.2179942, 2023.

Ternaris UG: Rosbags: Pure Python Library to Read, Modify, Convert, and Write Rosbag Files., https://gitlab.com/ternaris/rosbags, 2025.

Thomas, D.: Dirk-Thomas/Vcstool, https://github.com/dirk-thomas/vcstool, 2026.

ublox: ZED-F9R-01B, https://cdn.sparkfun.com/assets/d/4/3/f/4/ZED-F9R-01B_Datasheet_UBX-19054459.pdf, datasheet, 2023.

Van Alphen, R., Rains, K. C., Rodgers, M., Malservisi, R., and Dixon, T. H.: UAV-Based Wetland Monitoring: Multispectral and Lidar Fusion with Random Forest Classification, Drones, 8, 113, https://doi.org/10.3390/drones8030113, 2024.

Viametris: MS-96, https://viametris.com/ms-96/, 2025.

Výbošťok, J., Chudá, J., Tomčík, D., Gretsch, D., Tomaštík, J., Pełka, M., Bedkowski, J., Skladan, M., and Mokroš, M.: An Open and Novel Low-Cost Terrestrial Laser Scanner Prototype for Forest Monitoring, Sensors, 26, https://doi.org/10.3390/s26010063, 2025.

Watzenig, D. and Horn, M., eds.: Automated Driving: Safer and More Efficient Future Driving, Springer International Publishing, Cham, ISBN 978-3-319-31895-0, https://doi.org/10.1007/978-3-319-31895-0, 2017.

Xsens: MTi 630, https://www.mouser.fr/datasheet/2/1484/MTi_600_series_Datasheet-3193436.pdf, datasheet, 2020.

https://doi.org/10.5194/egusphere-2026-2492
Preprint. Discussion started: 10 June 2026

YellowScan: Surveyor Ultra, https://www.yellowscan.com/products/surveyor_ultra/, 2025.

Zhang, Y., Carballo, A., Yang, H., and Takeda, K.: Autonomous Driving in Adverse Weather Conditions: A Survey, arXiv:2112.08936 [cs], 2021.